A peer-reviewed version of this preprint was published in PeerJ on 24 May 2016.

Subramanian P, Jayapalan JJ, Abdul-Rahman PS, Arumugam M, Hashim OH. 2016. Temporal regulation of proteome profile in the fruit fly, *Drosophila melanogaster*. PeerJ 4:e2080
https://doi.org/10.7717/peerj.2080

Temporal regulation of proteome profile in the fruit fly, *Drosophila melanogaster*

Perumal Subramanian, Jaime J Jayapalan, Puteri Abdul-Rahman, Manjula Arumugam, Onn Hashim

Background. Diurnal rhythms of protein synthesis controlled by the biological clock underlie rhythmic physiology in the fruit fly, *Drosophila melanogaster*. Self-sustained autonomous circadian oscillations were documented all over the organs of the fly. In this study, we conducted a proteome-wide investigation of rhythmic protein accumulation in *D. melanogaster*. **Materials and Methods.** We have used the whole fly for the proteomic study as performed in typical proteotypic peptide (PTP) studies and followed the same protocol with trypsin digestion. Total protein collected from fly samples harvested at 4h intervals over the 24-h period were subjected to two dimensional (2-D) gel electrophoresis, trypsin digestion and MS/MS analysis. Protein spots/clusters were identified with MASCOT search engine and Swiss-Prot database. Expression of proteins was documented as percentage of volume contribution using the Image Master 2D Platinum software. **Results.** A total of 124 protein spots/clusters were identified using MS/MS analysis. A significant variation in the expression of 88 proteins over the 24-h period was observed. Our present results suggested that the synthesis/regulation of numerous proteins is regulated by the biological clock in *D. melanogaster*. Relatively higher number of proteins was upregulated during nighttime as compared to daytime. **Conclusion.** As these rhythmically varying proteins/enzymes involve in metabolism, muscle activities, ion channels, protein synthesis, redox homeostasis and apoptosis our results indicate that these cellular processes could be regulated at the level of temporal expression of protein profile.

PeerJ PrePrints | https://doi.org/10.7287/peerj.preprints.1677v1 | CC-BY 4.0 Open Access | rec: 23 Jan 2016, publ: 23 Jan 2016

Temporal regulation of proteome profile in the fruit fly, *Drosophila melanogaster*

Perumal Subramanian[1], Jaime Jacqueline Jayapalan[2], Puteri Shafinaz Abdul-Rahman[2,3], Manjula Arumugam[1] and Onn Haji Hashim[2,3]

[1]Department of Biochemistry and Biotechnology, Faculty of Science, Annamalai University, Chidambaram 608 002, Tamil Nadu, India

[2]University of Malaya Centre for Proteomics Research (UMCPR), Faculty of Medicine, University of Malaya, 50603 Kuala Lumpur, Malaysia

[3]Department of Molecular Medicine, Faculty of Medicine, University of Malaya, 50603 Kuala Lumpur, Malaysia

Corresponding author:

Perumal Subramanian
Professor
Department of Biochemistry and Biotechnology
Faculty of Science
Annamalai University
Chidambaram – 608 002
Tamil Nadu, India
Phone: +91 4144 239141 Extn: 210
E-mail: psub@rediffmail.com

ABSTRACT

Background. Diurnal rhythms of protein synthesis controlled by the biological clock underlie rhythmic physiology in the fruit fly, *Drosophila melanogaster*. Self-sustained autonomous circadian oscillations were documented all over the organs of the fly. In this study, we conducted a proteome-wide investigation of rhythmic protein accumulation in *D. melanogaster*.

Materials and Methods. We have used the whole fly for the proteomic study as performed in typical proteotypic peptide (PTP) studies and followed the same protocol with trypsin digestion. Total protein collected from fly samples harvested at 4h intervals over the 24-h period were subjected to two dimensional (2-D) gel electrophoresis, trypsin digestion and MS/MS analysis. Protein spots/clusters were identified with MASCOT search engine and Swiss-Prot database. Expression of proteins was documented as percentage of volume contribution using the Image Master 2D Platinum software.

Results. A total of 124 protein spots/clusters were identified using MS/MS analysis. A significant variation in the expression of 88 proteins over the 24-h period was observed. Our present results suggested that the synthesis/regulation of numerous proteins is regulated by the biological clock in *D. melanogaster*. Relatively higher number of proteins was upregulated during nighttime as compared to daytime.

Conclusion. As these rhythmically varying proteins/enzymes involve in metabolism, muscle activities, ion channels, protein synthesis, redox homeostasis and apoptosis our results indicate that these cellular processes could be regulated at the level of temporal expression of protein profile.

INTRODUCTION

A wide spectrum of physiological, cellular, biochemical, endocrinological and molecular functions in living systems display temporal (24-h) rhythms. As a consequence, the extent of biological processes regulated by biological clock vary from sleep-wake patterns, body temperature, activities of numerous enzymes, hormones, synthesis of nucleic acids and cell division (*Moore-Ede et al., 1982*). As numerous aspects of cell metabolism and cell division cycle are regulated by biological clock (*Asher & Schibler, 2011*; *Bass & Takashashi, 2010*) it could be easily hypothesized that proteome profile of a living organism could be circadian in nature.

Previous studies showed that 30% of mRNA transcripts exhibit circadian variation (*Luck et al., 2014*). The circadian regulation of posttranslational processes has been revealed by the studies of circadian rhythms of proteomes (*Robles et al., 2014*). There are previous reports that the cerebrospinal fluid (CSF) proteome would vary over the light-dark cycle (*Teixeira-Gomes et al., 2015*) and even seasonal regulation of CSF was documented (*Teixeira-Gomes et al., 2015*). Although, a lot of genes show coordinated rhythms in RNA synthesis, splicing and translation, numerous genes exhibit significant temporal disconnections between these functions (reviewed in *Beckwith & Yanovsky, 2014*). Hence, circadian oscillations represent a perfect system to comprehend how manifold transcriptional and post-transcriptional processes are integrated rhythmically to maximize fine-tunings of functions of organisms to environment cycles. The global level circadian proteome of whole mouse liver (inclusive of various functional parts – left and right triangular ligaments, fissure for ligamentum teres, fissure for ligamentum venosum, hepatic veins, *etc.,*) was investigated by *Reddy et al.,* (*2006*) which revealed a contrasting variation of protein profile between day and night.

Although rigorous research has been carried out on molecular genetics and developmental studies in the fruit fly, *Drosophila melanogaster*, little is known about the proteome of the fly. Nevertheless, *D. melanogaster* is an extensively used model system for circadian biology and a wide array of clock genes, clock controlled genes, temporally oscillating mRNA and behavioral processes have been investigated thus far. Proteomics is a central aspect in systems biology of the fruit fly that appends a distinctive dimension in investigating gene function and regulatory mechanisms. Hence, the temporal pattern of proteome profile would add useful information for further research and analysis. Search of PubMed

(http://www.ncbi.nlm.nih.gov/pubmed/) references illustrated that by the end of October 2015 articles on *Drosophila* proteomics constitute only 0.95% of all published papers on proteomics.

Conventional understanding has it that the circadian clock exists in the lateral neurons (in brain) of the fly (*Kaneko et al., 1997*). Intriguingly, brain-independent circadian oscillations (cells able to show self-maintained rhythmic outputs in numerous cellular processes) have been perceived in almost all peripheral tissues of *D. melanogaster* (*Hege et al., 1997; Plautz et al., 1997a, b*). For instance, the Malpighian tubules of the decapitated and of the non-decapitated flies bearing the *per-lacZ* reporter transgene, demonstrated the same circadian rhythms of β-galactosidase expression (*Hege et al., 1997*). *Plautz et al.,* (*1997a*) demonstrated the appearance, disappearance and reappearance of PERIOD protein in a rhythmic (24-h) pattern in the head, abdomen, thorax, legs and wings of the fly, indicating that numerous cellular processes all over the body of the fly are regulated by the temporally oscillating circadian clock gene, *period* all over the fly. Although, the existence of brain-independent circadian oscillations has been detected nearly 20 years ago, there has been no study on the integrated circadian proteome profile in the whole body of the fly. It is in this context, the present study has been carried out.

To investigate the global circadian transcriptional regulation in *D. melanogaser*, Rodriguez et al., (2013) separated nascent RNA from fly heads at six time points over 24h period (00:00, 04:00, 08:00, 12:00, 16:00 and 20:00 in 12:12h light-dark cycle) and their data specified a key role of posttranscriptional control to fly's circadian mRNA oscillation. Following the temporal schedule of *Rodriguez et al.,* (*2013*), in this study, we investigated the global pattern of temporal proteome (i) to complement the available data in fly literature (ii) as little is documented about the rhythmic buildup of proteins in *D. melanogaster* (*Mauvoisin et al., 2014*) and (iii) to reveal the integrated pattern/regulation of circadian proteome in the whole body of the fly.

MATERIALS AND METHODS

Drosophila culture and sample collection

D. melanogaster (wild type-Canton S) flies were maintained on medium comprising maize powder, sucrose, yeast and nepagin (anti-fungal agent) at 21 ± 2 ºC under 12h:12h (light:dark) phases. We have used the whole fly for the proteomic study as performed in typical proteotypic peptide (PTP) studies reported earlier (*Brunner et al., 2007*) and followed the same protocol with

trypsin digestion. The adult male flies (7 days old) were collected at 4 h intervals (*Rodriguez et al., 2013*) incessantly over the 24 h period (at 00:00, 04:00, 08:00, 12:00, 16:00 and 20:00). The flies collected at each time point (n=15) were suspended in sample solubilization solution (100 µL) containing equal volume of SDS (1%) and β-mercaptoethanol (5%) and were swiftly frozen in liquid nitrogen. The flies were homogenized and the homogenate was kept at –80 ºC until analysis. Then, the proteins were solubilized at 95 ºC in sample solubilization solution and vortexed. The miniature cuticle residues were sedimented by centrifugation at 8200 *g* (5 min). The solubilized proteins were precipitated in TCA (20%) in cold acetone (90%) along with dithiothreitol (DTT, 20 mM) on ice (*Jessie et al., 2008*).

Assay for protein estimation

The total protein content of fly homogenate was estimated (*Bradford, 1976*) after pre-treatment and re-solubilization of protein pellet with sodium hydroxide (0.2 M) and rehydration buffer (urea (7 M), thiourea (2 M), CHAPS (4%, 3-[(3-cholamidopropyl)dimethylammonio]-1-propanesulfonate) and bromophenol blue (0.002%)), respectively, as previously described (*Jessie et al., 2008*).

2-D gel electrophoresis (2DE) and silver staining

2DE was performed with 50 µg of precipitated (TCA/acetone) fly proteins. The proteins were incubated in rehydration buffer (urea (7 M), thiourea (2 M), CHAPS (4%), IPG buffer (pH 3-10 NL), DTT (65 mM) and bromophenol blue (0.002%)) at 25 °C for about 12 h and loaded onto 13 cm rehydrated precast immobilized dry strips (pH 3-10 non-linear, GE Healthcare BioSciences, Uppsala, Sweden). The strips were subjected to isoelectric focusing with EttanIPGhor 3 Isoelectric Focusing Unit (GE Healthcare, Uppsala, Sweden) for a total time of 20kV/h. Focused strips were equilibrated in Tris-HCl (1.5 M, pH 8.8 with urea (6 M), SDS (2%), glycerol (30%) and DTT (0.06 M)) for 20 min and subsequently incubated in a similar equilibration solution but containing iodoacetamide (4.5%) in lieu of DTT for 20 min. The equilibrated strips were then overlaid onto homogenous polyacrylamide gel (12.5%) and electrophoresis was carried following the protocol using the SE 600 Ruby Electrophoresis System and Power Supply-EPS601 (GE Healthcare), as reported earlier (*Jessie et al., 2008*). The 2DE gels were developed by silver staining (*Heukeshoven & Dernick, 1988*). All samples (at each time point) were examined independently in triplicate. A modified silver staining protocol was performed for

visualization of proteins well-suited for MALDI-ToF/ToF mass spectrometry (MS) investigation (*Yan et al., 2000*).

Image analysis

2DE gels (silver stained) were scanned using Imaging Densitometer GS690 (Bio-Rad Laboratories, Hercules, USA). Expression level of proteins was calculated in terms of percentage of volume contribution using the Image Master 2D Platinum software, version 7.0 (GE Healthcare Biosciences, Uppsala, Sweden) by selecting the particular spot of the 2DE, matching it with the same spot of another replicate (of the same time point) for which a matchset has been already created using the software. Cut-off parameters for this analysis were: Smooth - 2; Saliency – 1; Min area – 5 (*Jayapalan et al., 2012; 2013*).

Trypsin digestion and mass spectrometry

Identification of protein spots of interest was performed as described previously (*Jayapalan et al., 2012; 2013*). Further, spots were carefully excised from 2DE gels and destained with potassium ferricyanide (15 mM) and sodium thiosulfate (50 mM) for 20 min at about 20 °C. The proteins were reduced with 10 mM DTT (10 mM) and ammonium bicarbonate (100 mM) for 25 min, and alkylated with 55 mM iodoacetamide (55 mM) for 15 min, at 60 °C and in the dark, respectively. This was followed by subsequent washings with 50 and 100% acetonitrile (ACN, 50 and 100%) in 100 mM ammonium bicarbonate (100 mM), and dehydration of the gel plugs using vacuum centrifugation. The spots were digested with trypsin (6 ng/µl in ammonium bicarbonate solution (50 mM)) at 37 °C, for about 12 h. Peptides were extracted from the gels using ACN (50 and 100%), subsequently. Extracted peptides were lyophilized, treated with formic acid (0.1%) and desalted using ZipTip columns containing C^{18} reversed phase media (Millipore, Madison, USA). The sample peptide was mixed with α-cyano-4-hydroxycinamic acid (5 mg/ml) at a ratio of 1:1, and 0.7 µl of the mixture was immediately spotted onto an OptiToF 384-wellinsert and analysed using 5800 MALDI ToF/ToF analyser (ABSciex, Toronto, Canada).

Identification of proteins

The proteins in the spots/clusters were identified using the MASCOT search engine (*Jayapalan et al., 2012; 2013*). The MS data acquired was searched against *Drosophila melanogaster* in the Swiss-Prot database (last update: 21 April 2015, 3067 sequences) in accordance with the following selection parameters: enzyme-trypsin, missed cleavage – 1, variable modification – 2;

(i) carbamidomethylation of cysteine and (ii) oxidation of methionine, MS precursor ion mass tolerance – 100 ppm, MS/MS fragment ion tolerance -0.2 Da and inclusion of monoisotopic masses only.

Statistical analysis

The values of percentage of volume contribution were expressed in mean±SD. The Statistical Package for Social Sciences (SPSS) version 22.0 (IBM Corporation, New York, USA) was used to analyze the data. The test of homogeneity was employed to evaluate the sample distribution of the dataset. As at 04:00 and 20:00 maximum numbers of protein spots are expressed and identified the percentage of volume contribution of spots/clusters of these time points are compared with other time points. The Student's *t*-test was subsequently used (*Jayapalan et al., 2012*) to compare means of percentage of volume contribution of the spots (04:00 and 20:00) with other time points (individually) of all datasets that showed normal distribution. A p value of < 0.01 was deemed significant.

RESULTS

Representative 2DE profiles at 00:00, 04:00, 08:00, 12:00, 16:00 and 20:00 showed marked variations in the protein spots/clusters over the 24-h period (Fig. 1A – F). A total of 124 protein spots/clusters were identified by MS/MS analysis. Based on known or predictive functions the proteins are classified into 11 groups (Table 1). We found a substantial variation in the expression of significant number of proteins (88 Nos.) over the 24-h period (Table 2). Relatively higher number of proteins (45) was upregulated during nighttime as compared to daytime (43) (Fig. 2A and B). However, during daytime higher number of groups of proteins (metabolism, muscle activity, ion-channel/cellular transport, protein synthesis/folding/degradation, redox homeostasis, development and transcription) were upregulated as compared to nighttime (metabolism, muscle activity, heat shock proteins, protein sysnthesis/folding/degradation and apoptosis) indicating the complexity of temporal regulation of proteome profile. Matched peptides of 2 or more reflect a better confidence of the results (Table 1). The proteins which have significant variation in percentage of volume contribution in at least 2 time points are categorized into 9 groups (metabolism, muscle activity, ion-channel/cellular transport, heat shock proteins, protein synthesis/folding/degradation, redox homeostasis, apoptosis, development and transcription) (Table 2 and Fig. 3A – I). The percentage of volume contribution of all 124 protein spots/clusters are shown in Supplemental Table 1. We observed

multiple hits for single protein spot (eg., spot/cluster Nos. 57 and 200, 59, 104 and 135, 86 and 175 and 120 and 204). Further, a few protein spots were not resolved at all time points (Fig. 1A – F). These missing spots are not considered for analysis.

The enzymes involved in metabolism (6-phosphofructokinase, succinate dehydrogenase, N-glycanase, maltase H, vacuolar ATP synthase catalytic subunits A and B, enolase, ATP synthase subunits (α, β and D chain), fructose bisphosphate aldolase, arginine kinase, stellate protein CG33247 (protein kinase regulator), triosephosphate isomerase, protein l(2)37Cc (DOPA decarboxylase), inorganic pyrophosphatase, pyruvate kinase, phosphoglycerate kinase, glycerol-3-phosphate dehydrogenase, isocitrate dehydrogenase, thioredoxin reductase, alcohol dehydrogenase and cytochrome P450) showed significant variations over the 24-h period (Table 2 and Fig. 3A).

The other proteins/enzymes which show significant variation of expression at different time points include: (i) the proteins involved in muscular activities (various types of actin (88F, 57B, 5C, 79B, 87E and 42A), myosin regulatory light chain-2, synapse associated protein, ADP-ribosylation factor-8, tubulin α-3 chain and paramyosin), (ii) ion-channel/proteins involved in transport processes (calreticulin, tubulin β-1 chain, porin, ADP/ATP translocase and transient receptor potential locus C protein), (iii) types of heat shock proteins (82 kDa, 70 kDa, 60 kDa and heat shock factor protein), (iv) proteins associated with synthesis/folding/degradation (protein disulfide isomerase, furin-like protease, 40 S ribosomal protein SA and S12 and elongation fator 1α (EF-1α), (v) redox homeostasis (glutathione-S-transferase) (vi) apoptosis (caspase-8 precursor and thioredoxin peroxidase (also as antioxidant)), (vii) development (vitellogenin-2 precursor) and transcription (RNA helicase) (Table 2 and Fig. 3B – I).

Among the 88 proteins which exhibit temporal variation, the spot IDs which show different levels of expression at a minimum of any four time points are: 32, 42, 43, 46, 51, 59, 71, 100, 102, 115, 116, 121, 130, 152, 158, 161, 164, 171, 174, 176, 185, 187, 193, 194, 200 and 209. The enzymes involved in metabolism and muscular activities – fructose bisphosphate aldolase (187), arginine kinase (209), thioredoxin reductase I (161) and actin-87E (200) were upregulated during daytime and showed a lowest level of expression at 00:00. Further, the proteins/enzymes involved in various active cellular processes (40S ribosomal protein SA (121), ATP synthase subunit β (185), heat shock protein 70 kDa (43), vacuolar ATP synthase subunit B (51), actin-88F (59), 57B (174) and 87E (200), thioredoxin peroxidase (100), RNA helicase

(130), phosphoglycerate kinase (152), ADP-ribosylation factor-8 (158), and elongation factor-1α (164)) showed lowest level of expression at midnight (00:00), and their levels are upregulated during daytime. Conversely, the proteins involved in apoptosis and toxin metabolism (caspase-8 precursor (176) and cytochrome P450 (193)) were upregulated at 20:00 compared to daytime points.

DISCUSSION

Living organisms perform their functions according to the major environmental condition, light-dark cycle. Since, proteins and enzymes play vital roles in almost all the physiological functions of the body; the proper control of protein expression in a temporal manner is a crucial aspect of fundamental property of the organism. As a complex interplay of multiple processes involve in the generation of overt rhythms of multiple biological functions, it is obvious that numerous proteins vary their expression in a temporal manner in the body of the fly. Studies on global assessment of fly's circadian proteome confirmed the rhythmic nature of translation in *D. melanogaster* (*Huang et al., 2013*). However, it could be hypothesized that 'circadian proteome' is the outcome of regulatory stages at multiple steps of transcription and translation (RNA processing, posttranscriptional and posttranslational modifications). Conservation of circadian and clock controlled genes regulating similar pathways across various species, including *Drosophila* and mammals is well known (*Akhtar et al., 2002*). The data generated on cellular mechanisms in *Drosophila* could be applicable to humans, since majority of the regulatory mechanisms and signaling pathways are conserved between *Drosophila* and humans (*Rodriguez et al., 2013*).

Our investigation showed the identification of 124 protein spots in whole fly body of which 88 showed temporal variation in expression. Analogous to our study, *Rodriguez et al.,* (*2013*) recognized more than 130 cycling transcriptional units in *D. melanogaster* heads, of which nearly one-third (44) cycled significantly analogous to the results of our study. Among these 44, mRNAs of two genes (cytochrome P450 and glutathione-S-transferase) showed similar timings of peaks at 20:00 and 16:00 respectively with our protein expression pattern. There are no other similar proteins common to both studies. However, significant oscillations of several other proteins involved in metabolism, muscle activity, cellular transport, redox homeostasis, protein synthesis/folding/degradation, cell division and transcription were reported by *Rodriguez*

et al., (2013). Since they have studied the mRNA levels in heads and our study has been done in whole fly this difference could be attributed.

The circadian proteome profile of whole mouse liver revealed only about 20% of soluble proteins is under circadian regulation (*Reddy et al., 2006*). In addition, circadian proteome of suprachiasmatic nuclei (mammalian circadian pacemaker) showed that roughly 13% of soluble proteins show robust oscillations (*Deery et al., 2009*); all these studies suggest that only lower percentage of protein profile is under clock control as observed in our study. Further, *Deery et al.,* (*2009*) showed that 53 protein spots of 2DE demonstrated significant circadian profile in SCN (localized region in anterior hypothalamus of brain) proteome. More protein spots showed maximum expression during day (65%) than night (35%). However in our study (whole fly proteome), slightly higher number of protein spots were upregulated during nighttime than daytime.

Determination of composition of proteins in the whole body of fruit fly is an essential step toward understanding the regulation of various proteins as an integrated system. In the whole body of *D. melanogaster* many genes show coordinated circadian oscillations of expression and there are significant disconnections between the processes of transcription, post-transcriptional processing and protein synthesis (*Beckwith & Yanovsky, 2014*). Thus, the analysis of circadian pattern of proteome is useful in analyzing how many fold transcriptional and translational steps vary to maximize organismal adjustments over day and night. The rhythmic protein abundance observed in the study could be caused by rhythmic protein synthesis activity and rhythmic protein half-life. Further, an extensive circadian pattern of protein profile could arise owing to (i) circadian transcriptional regulation by clock transcriptional factors and co-regulators which act on a wide array of circadian clock-controlled genes (ccgs) (*Asher & Schibler, 2011*), (ii) due to circadian hormonal signaling to various types of cells (*Asher & Schibler, 2011*; *Luck et al., 2014*) and (iii) rhythmically distinct feeding patterns.

Our study revealed the integrated pattern/regulation of proteome in the body of the fly and it could be necessary for optimizing growth and fitness. In this study, observation of multiple hits for single protein spot could be due to (i) very close-localization of two different spots of proteins, (ii) isoforms of the same proteins with a very close mass and pI and (iii) post-translational modifications. Further, in some cases, a considerable variability in volume contribution of protein spots was observed (for example, 6-phosphofructokinase at 04:00 –

0.0168 ± 0.080 or enolase at 16:00 – 0.1206 ± 0.1163). This could be owing to minuscule variations in the pI levels of proteins, posttranslational modifications (like phosphorylation) and presence of isoforms of same proteins with a very close mass analysed in three replicates. The missing spots at certain time points (Fig. 1A – F) could indicate a circadian variation in the expression of proteins. The PERIOD protein is known to express only during daytime in neurons and tissues and is absent during nighttime (Plautz et al., 1997 a, b). In our study, in the whole fly homogenate, we could not identify the protein. The reason may be owing to the sensitivity of current techniques employed (2DE/MS/MS). A combination of high performance liquid chromatography and 2DE/MS/MS would be highly sensitive to analyse the temporal variation of PERIOD protein in the whole fly homogenate. As our temporally oscillating proteins are involved in metabolism, muscle activity, cellular transport, protein synthesis, apoptosis and development, a clock regulated release of various neurotransmitters regulating these functions (*Moller et al., 2010*) could also be suggested. Numerous genes involved in carbohydrate and amino acid metabolism including enzymes and membrane transporters were reported to be rhythmic (*Akhtar et al., 2002*). The present results showing diurnal upregulation of main enzymes of carbohydrate/amino acid metabolism (fructose bisphosphate aldolase, arginine kinase, ATP synthase subunit β, vacuolar ATP synthase subunit B, arginine kinase, phosphoglycerate kinase and thioredoxin reductase I) demonstrate the synchronous activation and inhibition of a set of enzymes of carbohydrate/amino acid metabolism. Further, the minimal level of expression numerous proteins suggest that several cellular, biochemical and physiological activities are low at midnight in the fruit fly. The 24-h variation may be an indirect outcome of circadian control of ingestion or under a direct circadian control, mediated by neural and endocrine entities (*Akhtar et al., 2002*), from the master clock, located in lateral neurons of the fly.

Of late, an extensive interconnection has been documented between the molecular circadian clock and the underlying biochemical pathways that regulate the bioenergetics of the organism. The scope includes the regulatory role played by coenzymes (NAD(P)+/NAD(P)H), reactive oxygen species (superoxide anion and hydrogen peroxide), antioxidants, and physiological events that modulate the redox state (feeding condition and circadian rhythms) in determining the timing capacity of the molecular circadian clock. Both the circadian timing system and the metabolic network are tightly interlinked regulating each other (*Mendez et al.,*

337 *2015*). Further, circadian clock gene transcription factors in metabolic tissues synchronize
338 metabolic fuel utilization and storage with alternating durations of feeding and fasting parallel to
339 the rest–activity cycle (*Peek et al., 2015*).

340 Recent evidences suggest the temporal (confined to the evening and early night phaes)
341 accrual of yolk proteins in the seminal vesicles of *D. melanogaster* (*Majewska et al., 2014*).
342 While the mechanisms of input pathways to the central circadian clock and the core circadian
343 clock (lateral neurons in *D. melanogaster*) has been extensively known, the processes that
344 regulate the circadian output pathways (which result in the circadian proteome profile, as one of
345 the components) are poorly understood. Recent genome-wide studies in many organisms
346 suggested extensive translational regulation by circadian clock could mainly contribute to the
347 temporal protein profile, despite the robust mRNA rhythms observed (*Montenegro-Montero &*
348 *Larrondo, 2015*).

349 Previous studies have shown that several genes encoding cytoskeleton components are
350 under circadian control and they showed distinct oscillations of mRNA and protein synthesis of
351 these genes (*Akhtar et al., 2002*). The cytochrome P450 constitute a superfamily of
352 monooxygenase enzymes involved in detoxification and circadian oscillations of cytochrome
353 P450 genes were reported (*Akhtar et al., 2002*) corroborating our results. Among the 23 fast
354 skeletal muscle myosin genes, *myh_tc*, *myh_n1*, *myh_n4*, *myo18a_2*, and *myo18b_2* showed
355 circadian rhythmic expression and possess many circadian-related transcription factor binding
356 sites (Creb, Mef2 and E-box motifs) within their recognized promoter regions. In addition, the
357 circadian expression of these 5 *myosin* genes that are robustly correlated with the transcription
358 pattern of clock genes in fast skeletal muscle (*Lazado et al., 2014*). *Murphy et al.,* (*2014*)
359 reported significant interaction between circadian time and exercise for muscle genes *MYF6,*
360 *UCP3, MYOD1* and *PDK4*. Hence, the circadian pattern of muscle proteins is expected and to
361 our best knowledge this is the first report on the circadian expression of a set of muscle related
362 proteins, in *D. melanogaster*.

363 As the proteome of the whole fly temporally vary in multiple biological processes
364 including metabolism, muscle activities, cellular transport, apoptosis etc., our results indicate that
365 a wide range of physiological/cellular processes are fine tuned by the rhythmic expression of
366 protein profile. Although, the tissue specific expression of proteins and the coordination of
367 protein regulation in various tissues of the fly could not be analysed in this study, potential

avenues of future research on the temporal regulation of intracellular localization of proteins, exploration of rhythmically varying proteins in specific tissue types are wide open.

ACKNOWLEDGEMENTS

Visiting Professorship to Perumal Subramanian at Department of Molecular Medicine, University of Malaya is gratefully acknowledged. Wild type (Cantos S) *Drosophila melanogaster* flies were kindly provided by Rakesh Mishra, Senior Scientist, Centre for Cellular and Molecular Biology, Hyderabad, India.

Supplemental Table

Supplemental Table 1 for this article can be found online at

REFERENCES

Akhtar RA, Reddy AB, Maywood ES, Clayton JD, King VM, Smith AG, Gant TW, Hastings MH, Kyriacou CP. 2002. Circadian cycling of the mouse liver transcriptome, as revealed by cDNA microarray, is driven by the suprachiasmatic nucleus. *Current Biology* **12:**540-550.

Asher G, Schibler U. 2011. Crosstalk between components of circadian and metabolic cycles in mammals. *Cell Metabolism* **13:**125-137. DOI: 10.1016/j.cmet.2011.01.006.

Bass J, Takahashi JS. 2010. Circadian integration of metabolism and energetics. *Science* **330:**1349-1354. DOI: 10.1126/science.1195027.

Beckwith EJ, Yanovsky MJ. 2014. Circadian regulation of gene expression: At the crossroads of transcriptional and post-transcriptional regulatory networks. *Current Opinion in Genetics and Development* **27:**35-42. DOI: 10.1016/j.gde.2014.03.007.

Bradford MM. 1976. A rapid and sensitive method for the quantitation of microgram quantities of protein utilizing the principle of protein-dye binding. *Analytical Biochemistry* **72:**248-254.

Brunner E, Ahrens CH, Mohanty S, Baetschmann H, Loevenich S, Potthast F, Deutsch EW, Panse C, de Lichtenberg U, Rinner O, Lee H, Pedrioli PGA, Malmstrom J, Koehler K, Schrimpf S, Krijgsveld J, Kregenow F, Heck AJR, Hafen E, Schlapbach R, Aebersold R. 2007. A high-quality catalog of the *Drosophila melanogaster* proteome. *Nature Biotechnology* **25:**576-583. DOI: 10.1038/nbt1300.

Deery MJ, Maywood ES, Chesham JE, Sladek M, Karp NA, Green EW, Charles PD, Reddy AB, Kyriacou CP, Lilley KS, Hastings MH. 2009. Proteomic analysis reveals the role of synaptic vesicle cycling in sustaining the suprachiasmatic circadian clock. *Current Biology* **19:**2031-2036. DOI: 10.1016/j.cub.2009.10.024.

Hege DM, Stanewsky R, Hall JC, Giebultowicz JM. 1997. Rhythmic expression of a PER-reporter in the Malpighian tubules of decapitated *Drosophila*: evidence for a brain-independent circadian clock. *Journal of Biological Rhythms* **12:**300-308.

Heukeshoven J, Dernick R. 1988. Improved silver staining procedure for fast staining in PhastSystem Development Unit. I. Staining of sodium dodecyl sulfate gels. *Electrophoresis* **9:**28-32. DOI: 10.1002/elps.1150090106.

Huang Y, Ainsley JA, Reijmers LG, Jackson FR. 2013. Translational profiling of clock cells reveals circadianly synchronized protein synthesis. *PLoS Biology* **11:**e1001703. DOI: 10.1371/journal.pbio.1001703.

Jayapalan JJ, Ng KL, Razack AH, Hashim OH. 2012. Identification of potential complementary serum biomarkers to differentiate prostate cancer from benign prostatic hyperplasia using gel- and lectin-based proteomics analyses. *Electrophoresis* **33:**1855-1862. DOI: 10.1002/elps.201100608.

Jayapalan JJ, Ng KL, Shuib AS, Razack AH, Hashim OH. 2013. Urine of patients with early prostate cancer contains lower levels of light chain fragments of inter-alpha-trypsin inhibitor and saposin B but increased expression of an inter-alpha-trypsin inhibitor heavy chain 4 fragment. *Electrophoresis* **34:**1663-1669. DOI: 10.1002/elps.201200583.

Jessie K, Hashim OH, Rahim ZHA. 2008. Protein precipitation method for salivary proteins and rehydration buffer for two-dimensional electrophoresis. *Biotechnology* **7:**686-693. DOI: 10.3923/biotech.2008.686.693

Kaneko M, Helfrich-Forster C, Hall JC. 1997. Spatial and temporal expression of the period and timeless genes in the developing nervous system of *Drosophila*: Newly identified pacemaker candidates and novel features of clock gene product cycling. *Journal of Neuroscience* **17:**6745-6760.

Lazado CC, Nagasawa K, Babiak I, Kumaratunga HP, Fernandes JM. 2014. Circadian rhythmicity and photic plasticity of myosin gene transcription in fast skeletal muscle of Atlantic cod (*Gadus morhua*). *Marine Genomics* 18 Pt **A:**21-29. DOI: 10.1016/j.margen.2014.04.011.

Lück S, Thurley K, Thaben Paul F, Westermark Pål O. 2014. Rhythmic degradation explains and unifies circadian transcriptome and proteome data. *Cell Reports* **9:**741-751. DOI: 10.1016/j.celrep.2014.09.021.

Majewska MM, Suszczynska A, Kotwica-Rolinska J, Czerwik T, Paterczyk B, Polanska MA, Bernatowicz P, Bebas P. 2014. Yolk proteins in the male reproductive system of the fruit fly *Drosophila melanogaster*: Spatial and temporal patterns of expression. *Insect Biochemistry and Molecular Biology* 47:23-35. DOI: 10.1016/j.ibmb.2014.02.001.

Mauvoisin D, Wang J, Jouffe C, Martin E, Atger F, Waridel P, Quadroni M, Gachon F, Naef F. 2014. Circadian clock-dependent and -independent rhythmic proteomes

implement distinct diurnal functions in mouse liver. *Proceedings of the National Academy of Sciences of the United States of America* **111:**167-172. DOI: 10.1073/pnas.1314066111.

Mendez I, Vazquez-Martinez O, Hernandez-Munoz R, Valente-Godinez H, Diaz-Munoz M. 2015. Redox regulation and pro-oxidant reactions in the physiology of circadian systems. *Biochimie*. DOI: 10.1016/j.biochi.2015.04.014.

Moller M, Lund-Andersen C, Rovsing L, Sparre T, Bache N, Roepstorff P, Vorum H. 2010. Proteomics of the photoneuroendocrine circadian system of the brain. *Mass Spectrometry Reviews* **29:**313-325. DOI: 10.1002/mas.20237.

Montenegro-Montero A, Larrondo LF. 2015. In the driver's seat: The case for transcriptional regulation and coupling as relevant determinants of the circadian transcriptome and proteome in eukaryotes. *Journal of Biological Rhythms*. DOI: 10.1177/0748730415607321.

Moore-Ede MC, Sulzman FM, Fuller CA. 1982. *The clocks that time us: Physiology of the circadian timing system.* Cambridge: Harvard University Press.

Murphy BA, Wagner AL, McGlynn OF, Kharazyan F, Browne JA, Elliott JA. 2014. Exercise influences circadian gene expression in equine skeletal muscle. *The Veterinary Journal* **201:**39-45. DOI: 10.1016/j.tvjl.2014.03.028.

Peek CB, Ramsey KM, Levine DC, Marcheva B, Perelis M, Bass J. 2015. Circadian regulation of cellular physiology. *Methods in Enzymology* **552:**165-184. DOI: 10.1016/bs.mie.2014.10.006.

Plautz JD, Kaneko M, Hall JC, Kay SA. 1997a. Independent photoreceptive circadian clocks throughout *Drosophila*. *Science* **278:**1632-1635.

Plautz JD, Straume M, Stanewsky R, Jamison CF, Brandes C, Dowse HB, Hall JC, Kay SA. 1997b. Quantitative analysis of *Drosophila* period gene transcription in living animals. *Journal of Biological Rhythms* **12:**204-217.

Reddy AB, Karp NA, Maywood ES, Sage EA, Deery M, O'Neill JS, Wong GKY, Chesham J, Odell M, Lilley KS, Kyriacou CP, Hastings MH. 2006. Circadian orchestration of the hepatic proteome. *Current Biology* **16:**1107-1115. DOI: 10.1016/j.cub.2006.04.026.

Robles MS, Cox J, Mann M. 2014. In-vivo quantitative proteomics reveals a key contribution of post-transcriptional mechanisms to the circadian regulation of liver metabolism. *PLoS Genetics* **10:**e1004047. DOI: 10.1371/journal.pgen.1004047.

Rodriguez J, Tang C-HA, Khodor YL, Vodala S, Menet JS, Rosbash M. 2013. Nascent-Seq analysis of *Drosophila* cycling gene expression. *Proceedings of the National Academy of Sciences of the United States of America* **110:**E275-E284. DOI: 10.1073/pnas.1219969110.

Teixeira-Gomes AP, Harichaux G, Gennetay D, Skipor J, Thiery JC, Labas V, Dufourny L. 2015. Photoperiod affects the cerebrospinal fluid proteome: a comparison between short day- and long day-treated ewes. *Domestic Animal Endocrinology* **53:**1-8. DOI: 10.1016/j.domaniend.2015.04.003.

Yan JX, Wait R, Berkelman T, Harry RA, Westbrook JA, Wheeler CH, Dunn MJ. 2000. A modified silver staining protocol for visualization of proteins compatible with matrix-assisted laser desorption/ionization and electrospray ionization-mass spectrometry. *Electrophoresis* **21:**3666-3672. DOI: 10.1002/1522-2683.

Figure 1(on next page)

Figure 1 Representative 2DE photographs.

Figure 1 Representative 2DE photographs of proteome profile of *Drosophila melanogaster* at 4-h intervals over a period of 24-h. The protein spots/cluters are labeled in black (or) white for easy visualization. (A) – 00:00, (B) – 04:00, (C) – 08:00, (D) – 12:00, (E) – 16:00 and (F) – 20:00. At each time point, 2DE was performed in triplicate. Expression levels of the spots/clusters are designated as percentage of volume contribution using the Image Master 2D Platinum software, version 7.0.

Figure 1

(A)

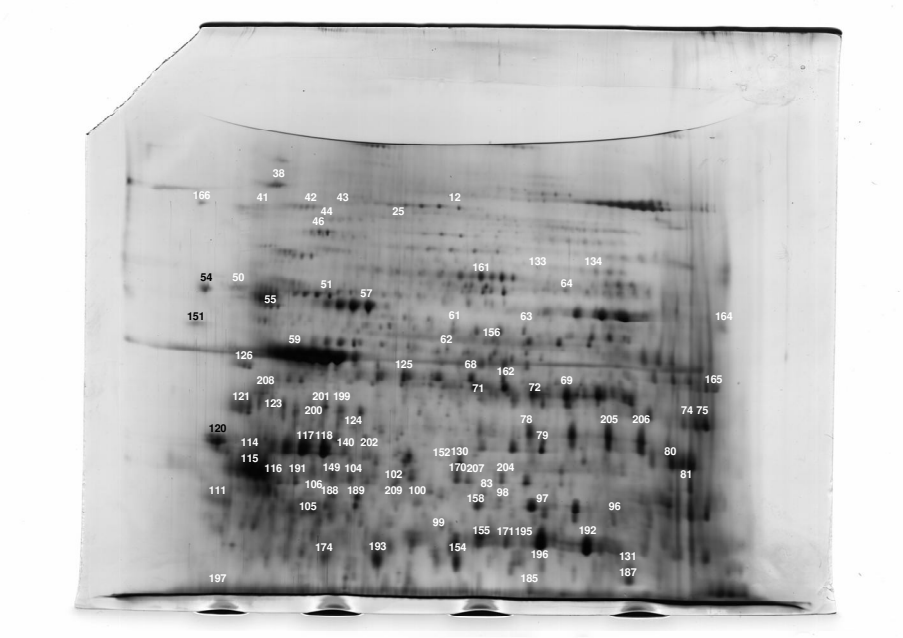

(B)

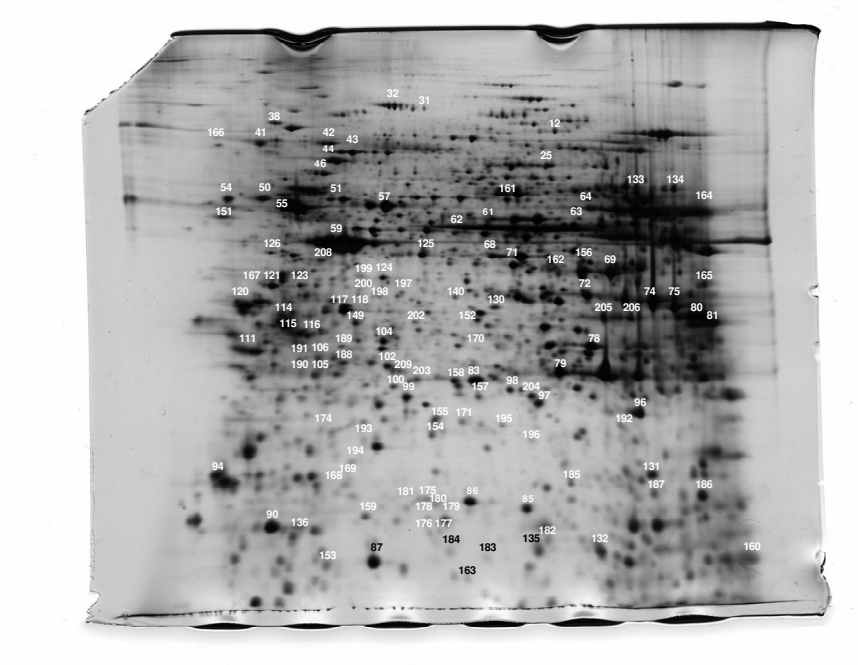

(C)

(D)

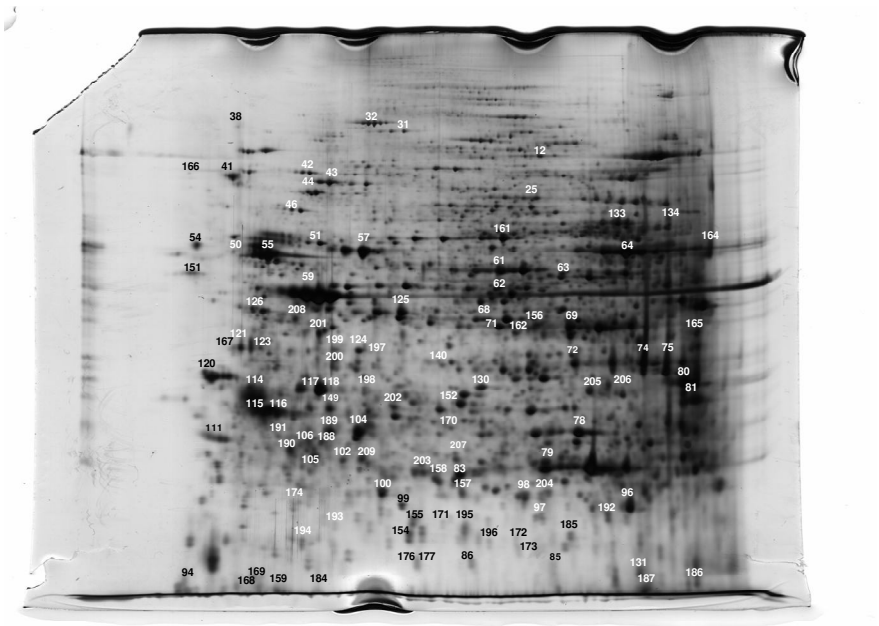

(E)

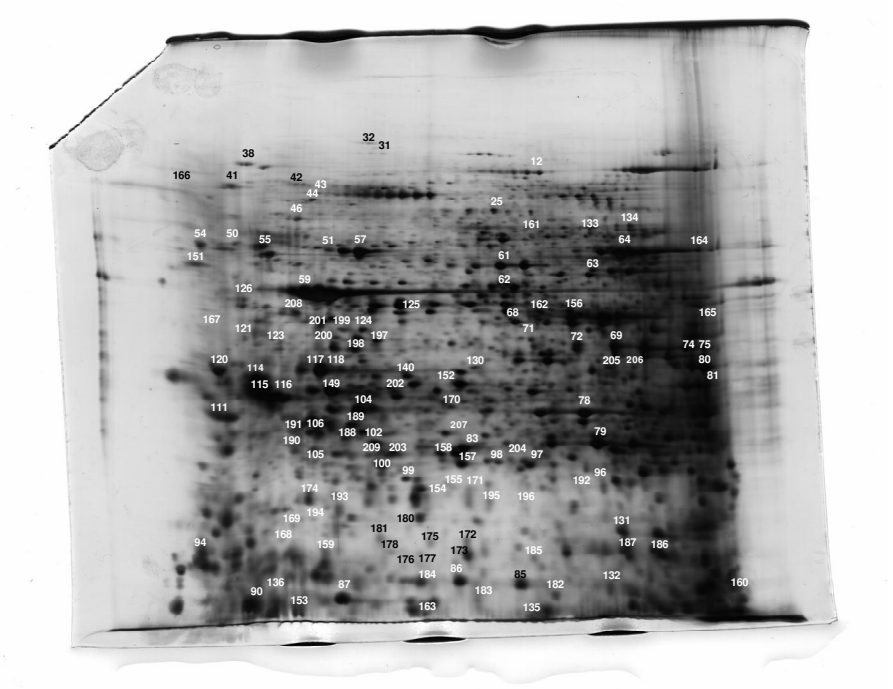

(F)

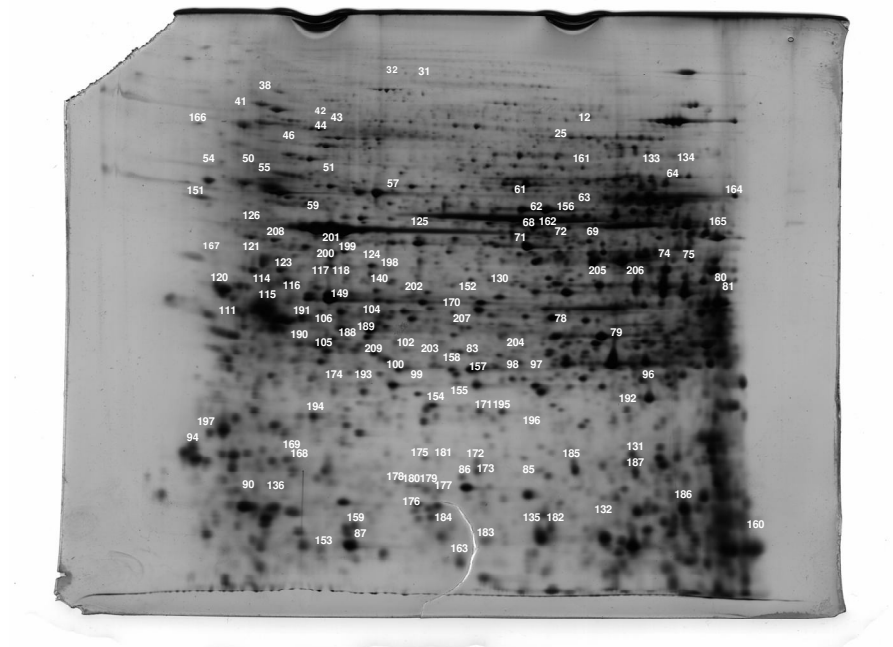

Figure 2(on next page)

Figure 2 Contribution of protein groups over the 24-h period.

Figure 2 (A) The contribution of upregulated proteins of each group (I – metabolism, II – muscle activity, III – ion-channel/cellular transport, IV – protein synthesis/folding/degradation, V – redox homeostasis, VI – development and VII - transcription) during daytime (representing 08:00, 12:00 and 16:00) is represented. (B) The contribution of upregulated proteins of each group (I – metabolism, II – muscle activity, III – heat shock proteins, IV – protein synthesis/folding/degradation and V – apoptosis) during nighttime (representing 20:00, 00:00 and 04:00) is represented. See Table 2 for further details.

Figure 2

(A)

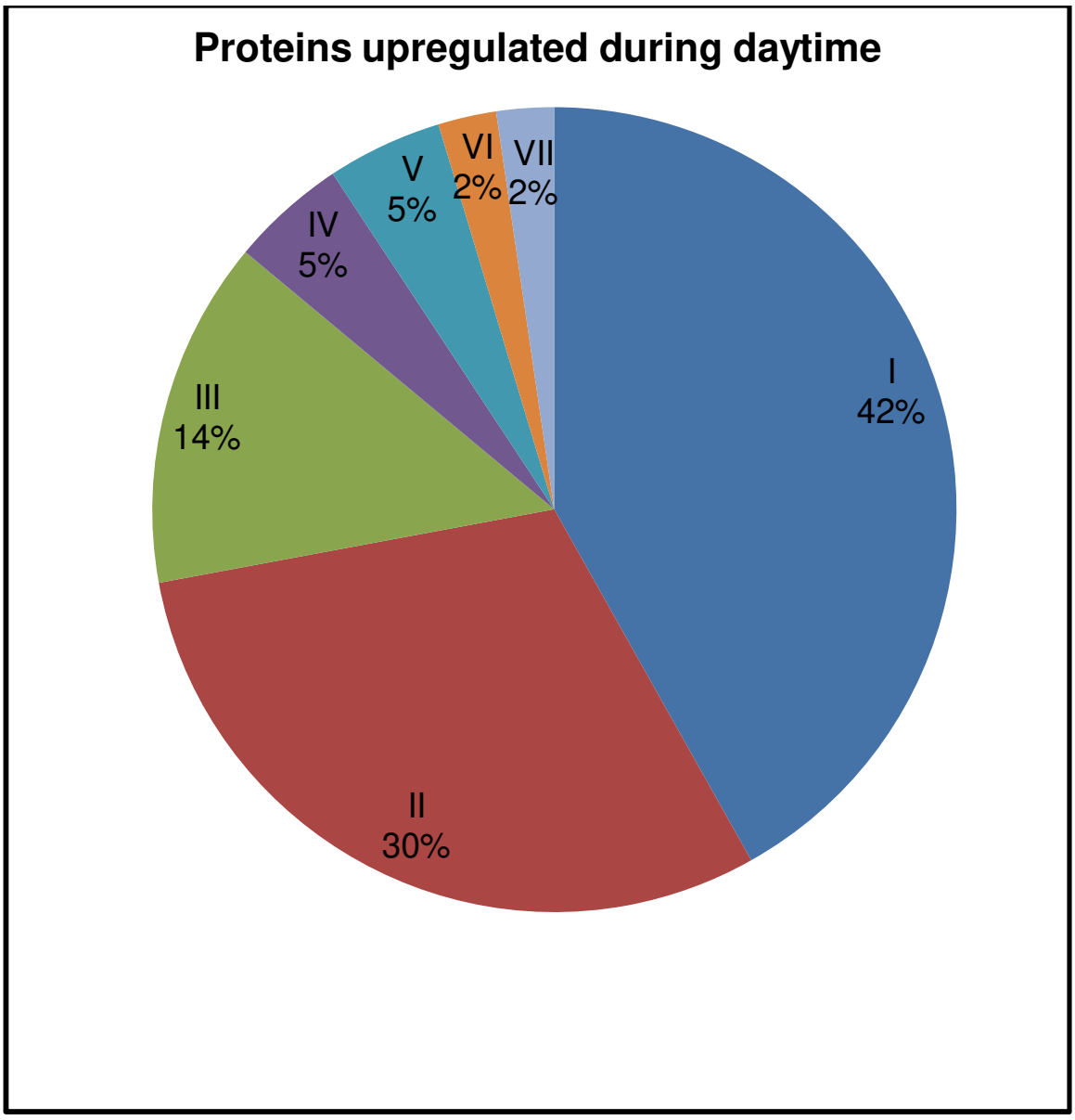

PeerJ PrePrints | https://doi.org/10.7287/peerj.preprints.1677v1 | CC-BY 4.0 Open Access | rec: 23 Jan 2016, publ: 23 Jan 2016

(B)

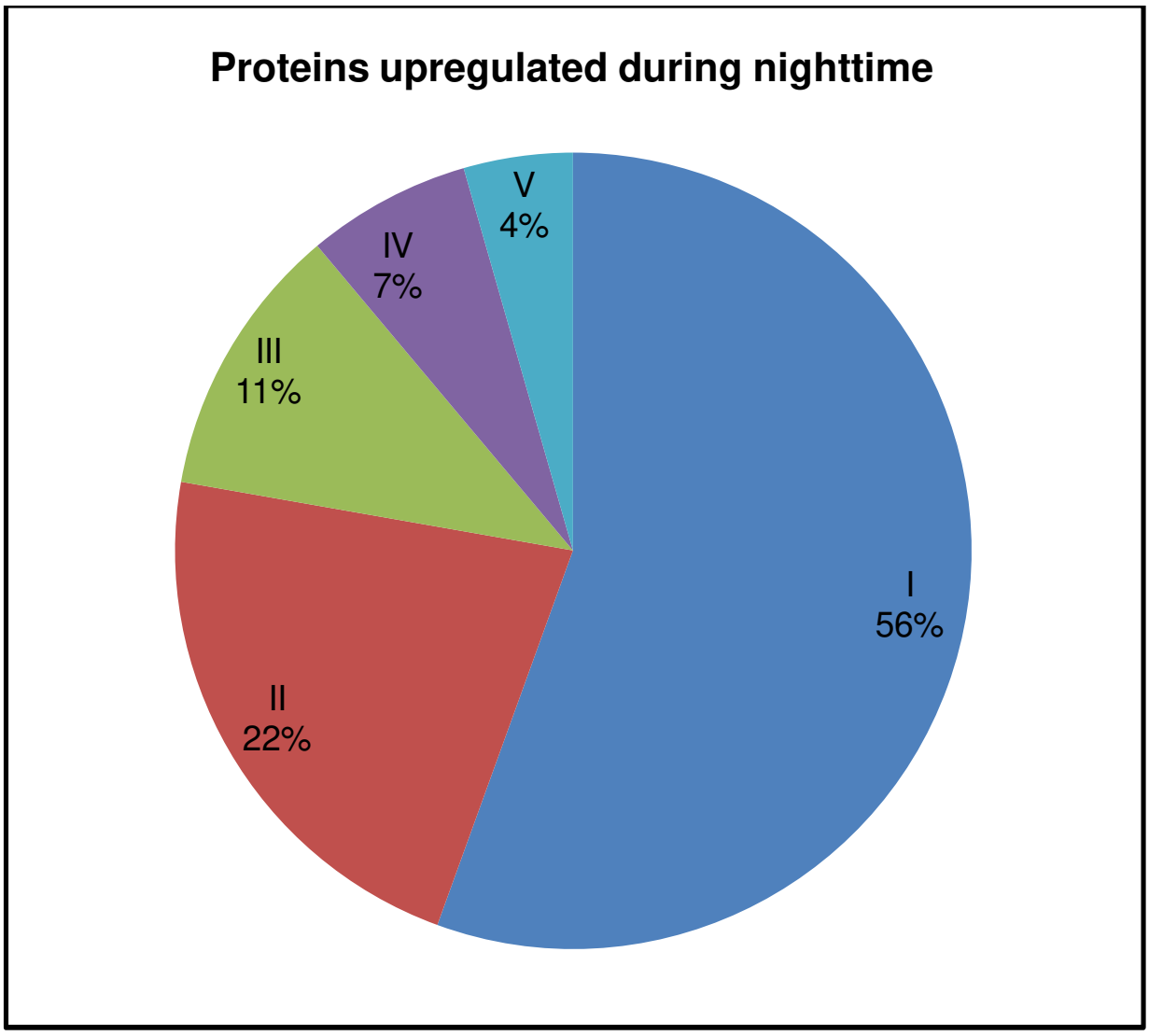

PeerJ PrePrints | https://doi.org/10.7287/peerj.preprints.1677v1 | CC-BY 4.0 Open Access | rec: 23 Jan 2016, publ: 23 Jan 2016

Figure 3(on next page)

Figure 3 Temporal variation in expression level of proteins.

Figure 3 Protein level variations (as percentage of volume contribution) of the groups across 24-h period are shown. The mean values of percentage of volume contribution are plotted for easy visualization. The corresponding SD values are given in Table 2. The proteins which show expression at all time points are represented and protein spot/cluster numbers are given in the figure. See Table 2 for further details. (A) – metabolism, (B) – muscle activity, (C) – ion-channel/cellular transport, (D) – heat shock proteins, (E) – protein synthesis/folding/degradation, (F) – redox homeostasis, (G) – apoptosis, (H) – development and (I) – transcription.

Figure 3

(A)

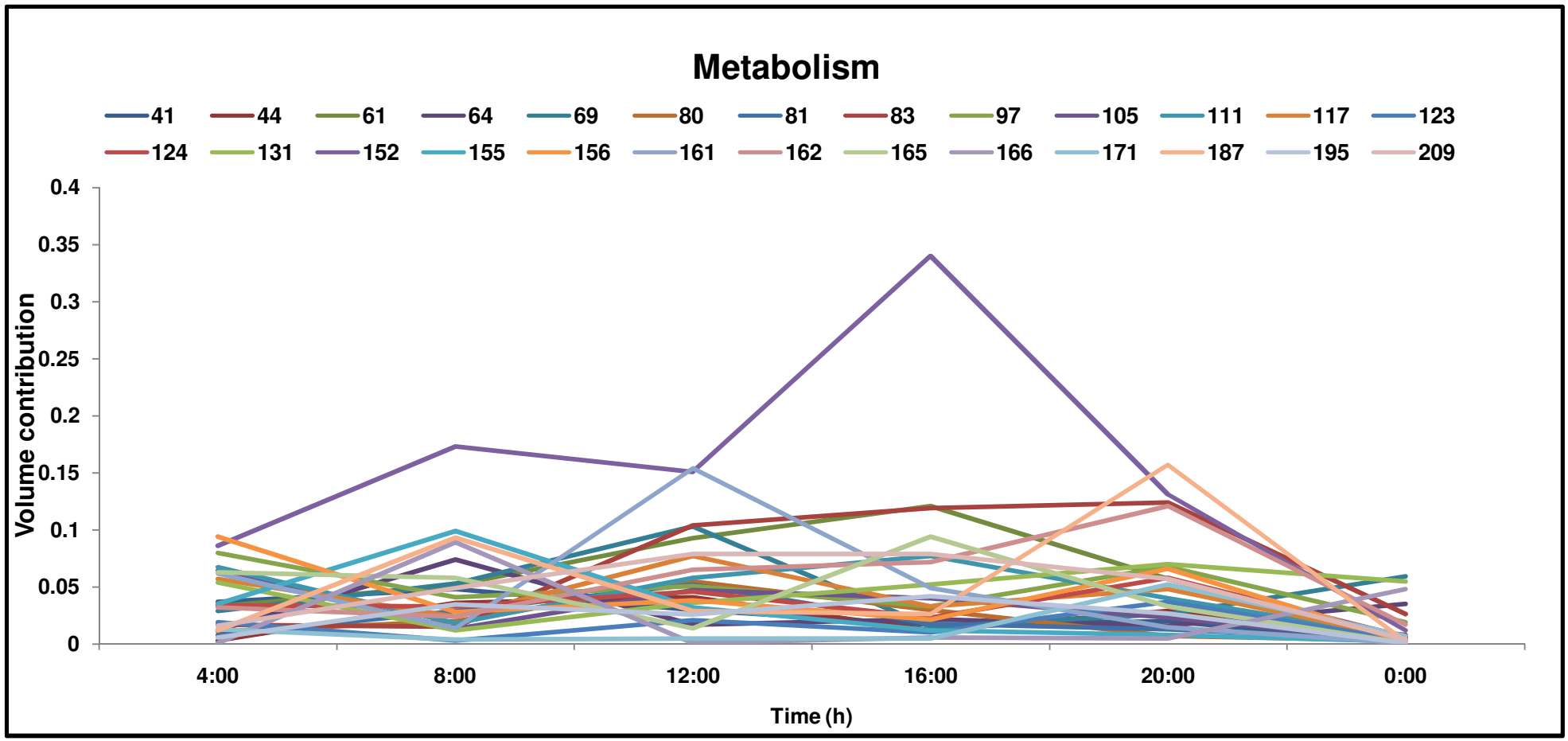

PeerJ PrePrints | https://doi.org/10.7287/peerj.preprints.1677v1 | CC-BY 4.0 Open Access | rec: 23 Jan 2016, publ: 23 Jan 2016

(B)

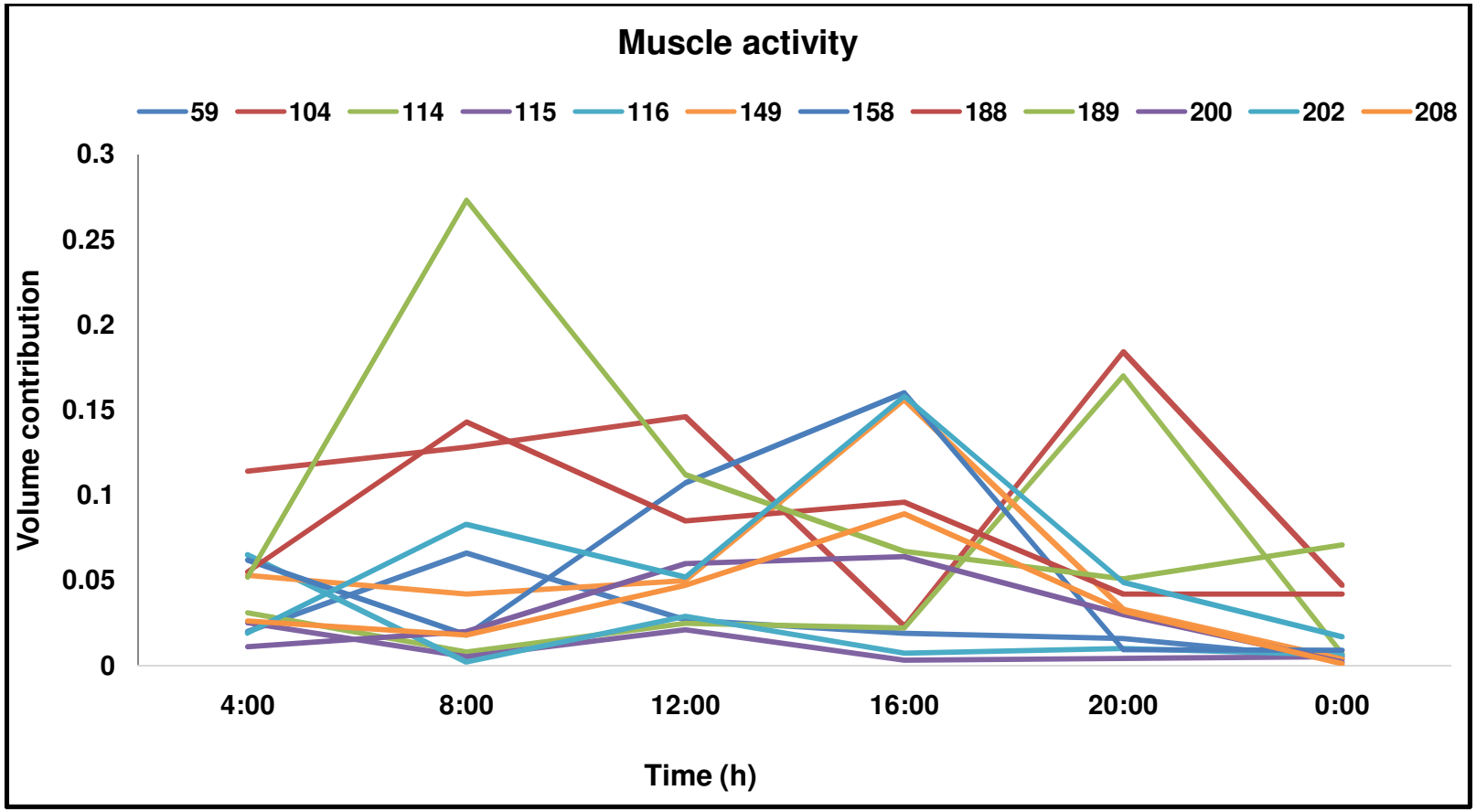

PeerJ PrePrints | https://doi.org/10.7287/peerj.preprints.1677v1 | CC-BY 4.0 Open Access | rec: 23 Jan 2016, publ: 23 Jan 2016

(C)

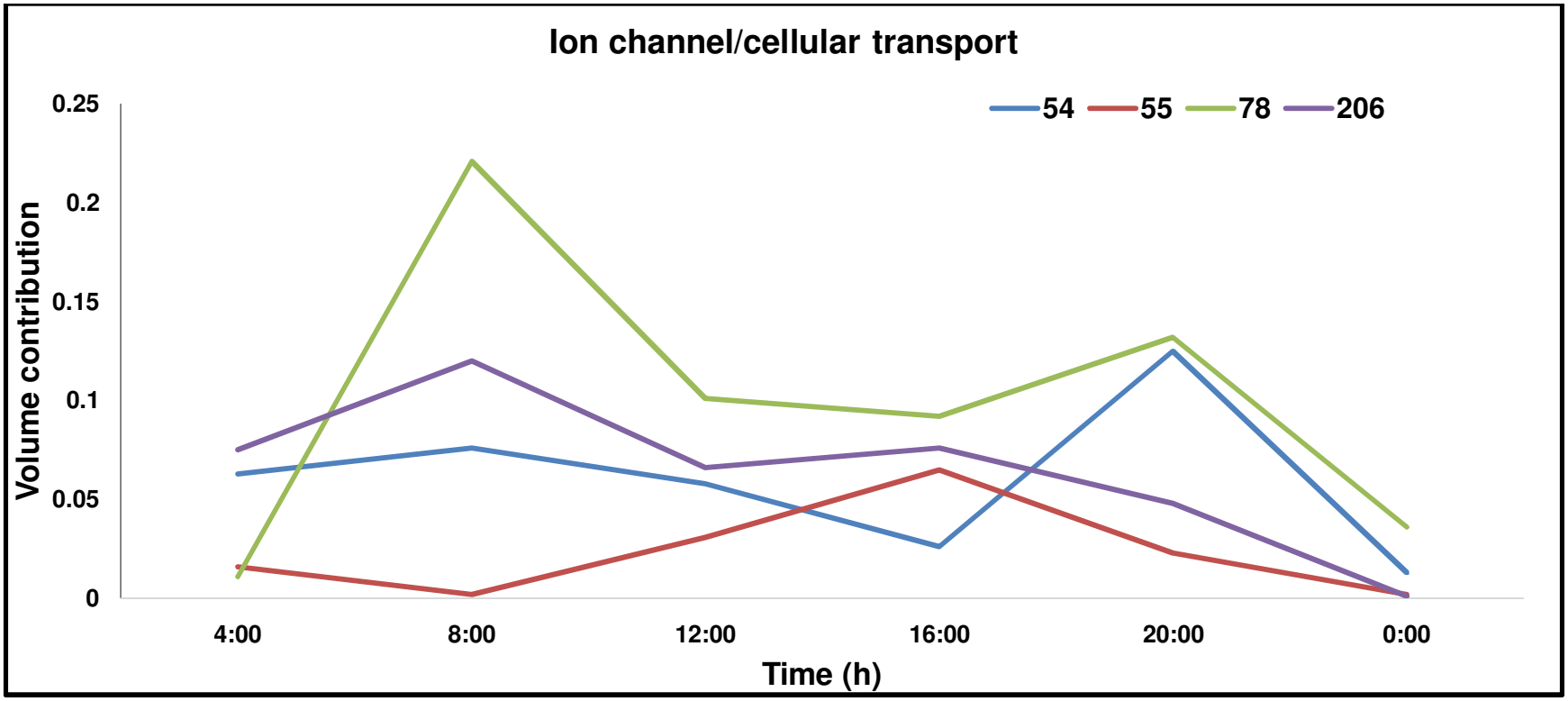

PeerJ PrePrints | https://doi.org/10.7287/peerj.preprints.1677v1 | CC-BY 4.0 Open Access | rec: 23 Jan 2016, publ: 23 Jan 2016

(D)

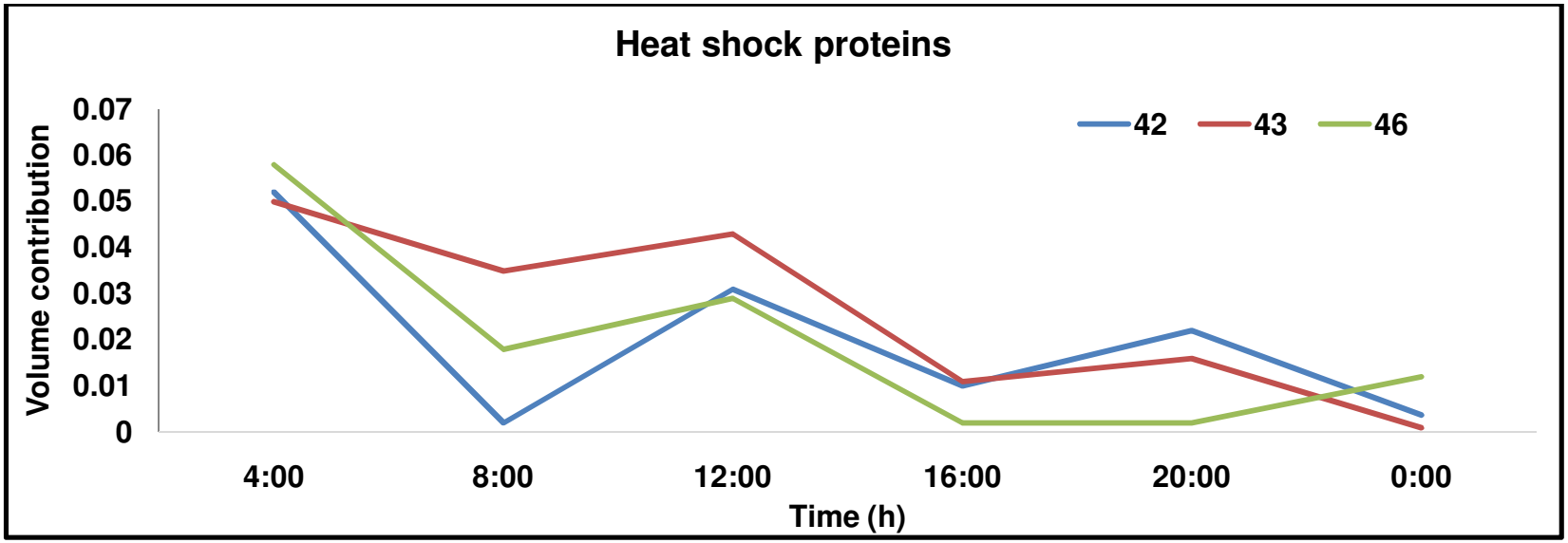

PeerJ PrePrints | https://doi.org/10.7287/peerj.preprints.1677v1 | CC-BY 4.0 Open Access | rec: 23 Jan 2016, publ: 23 Jan 2016

(E)

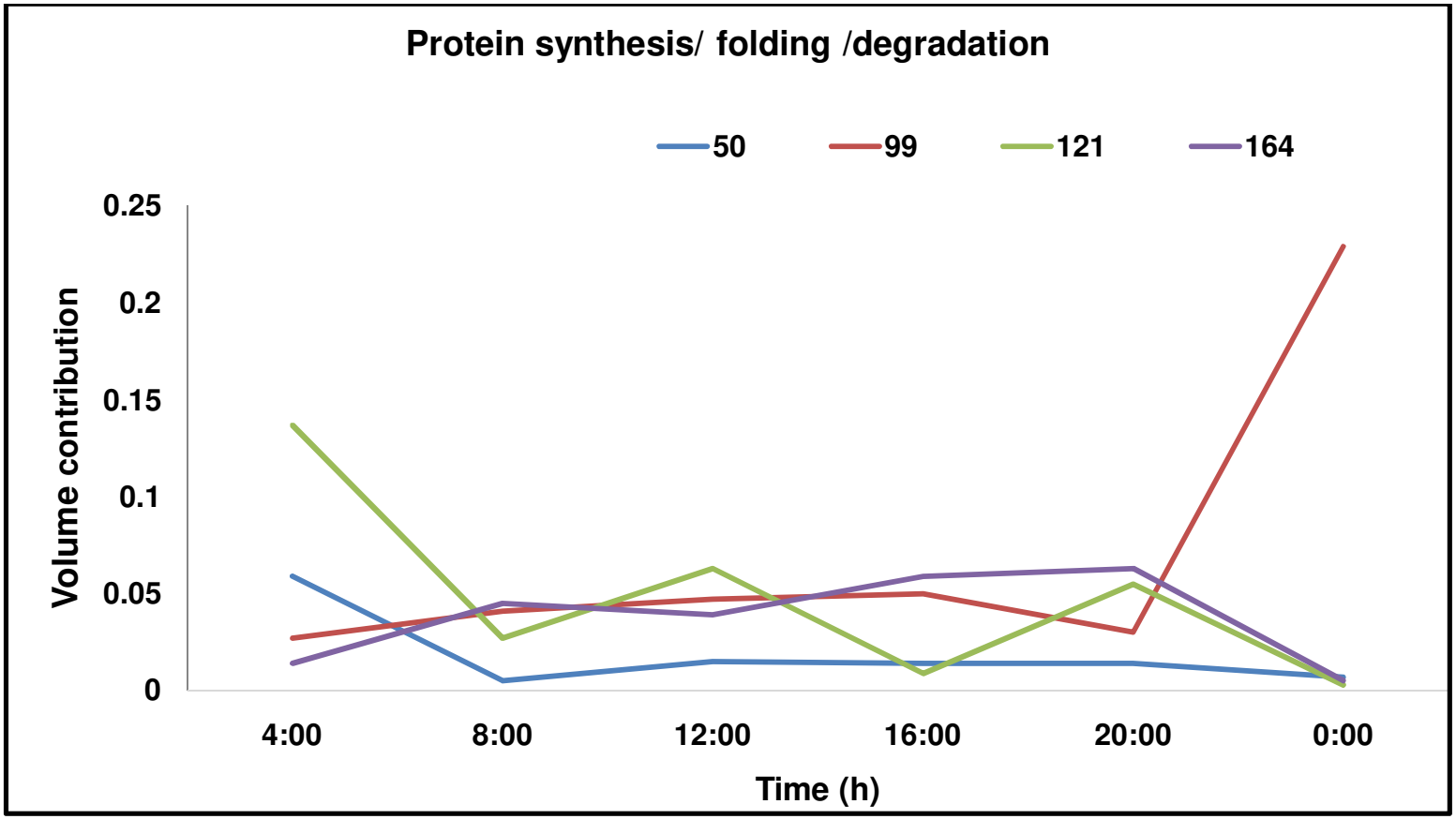

PeerJ PrePrints | https://doi.org/10.7287/peerj.preprints.1677v1 | CC-BY 4.0 Open Access | rec: 23 Jan 2016, publ: 23 Jan 2016

(F)

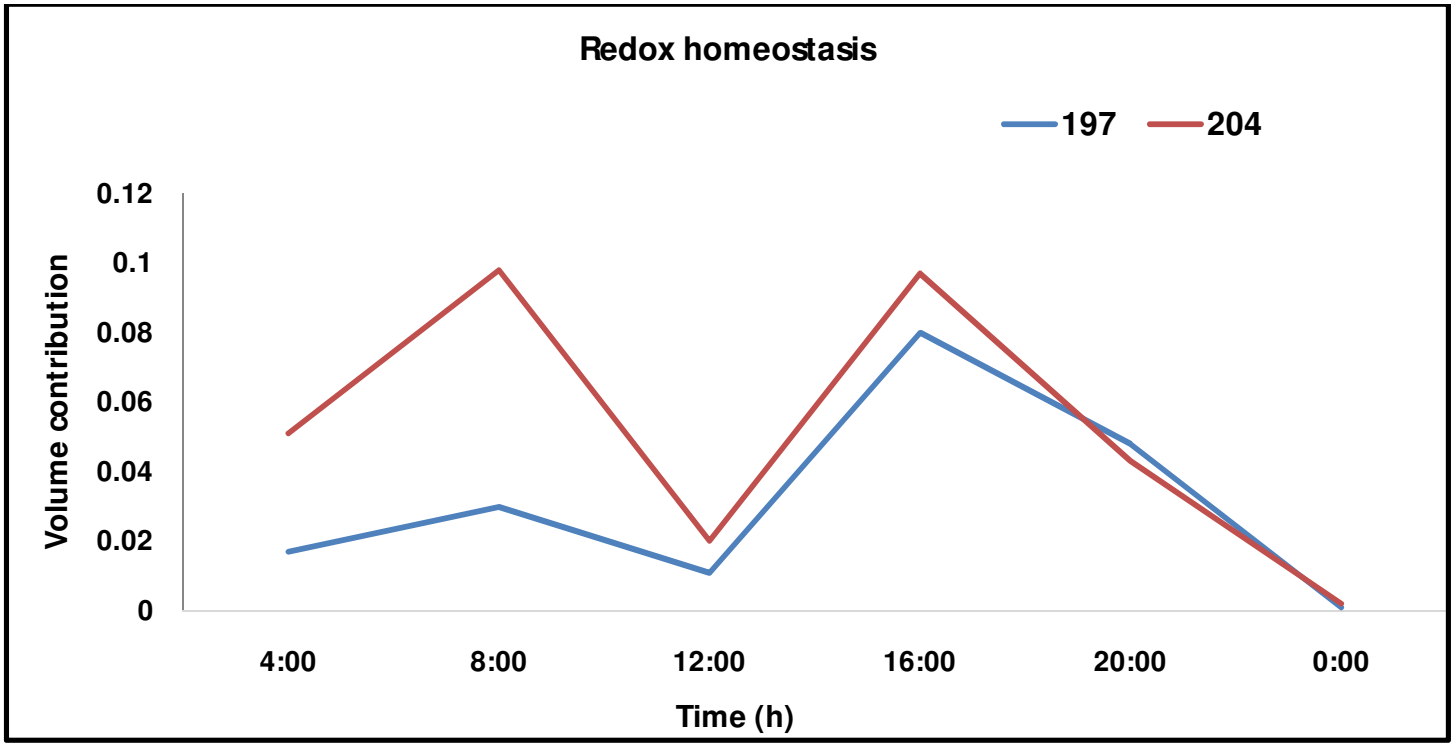

PeerJ PrePrints | https://doi.org/10.7287/peerj.preprints.1677v1 | CC-BY 4.0 Open Access | rec: 23 Jan 2016, publ: 23 Jan 2016

(G)

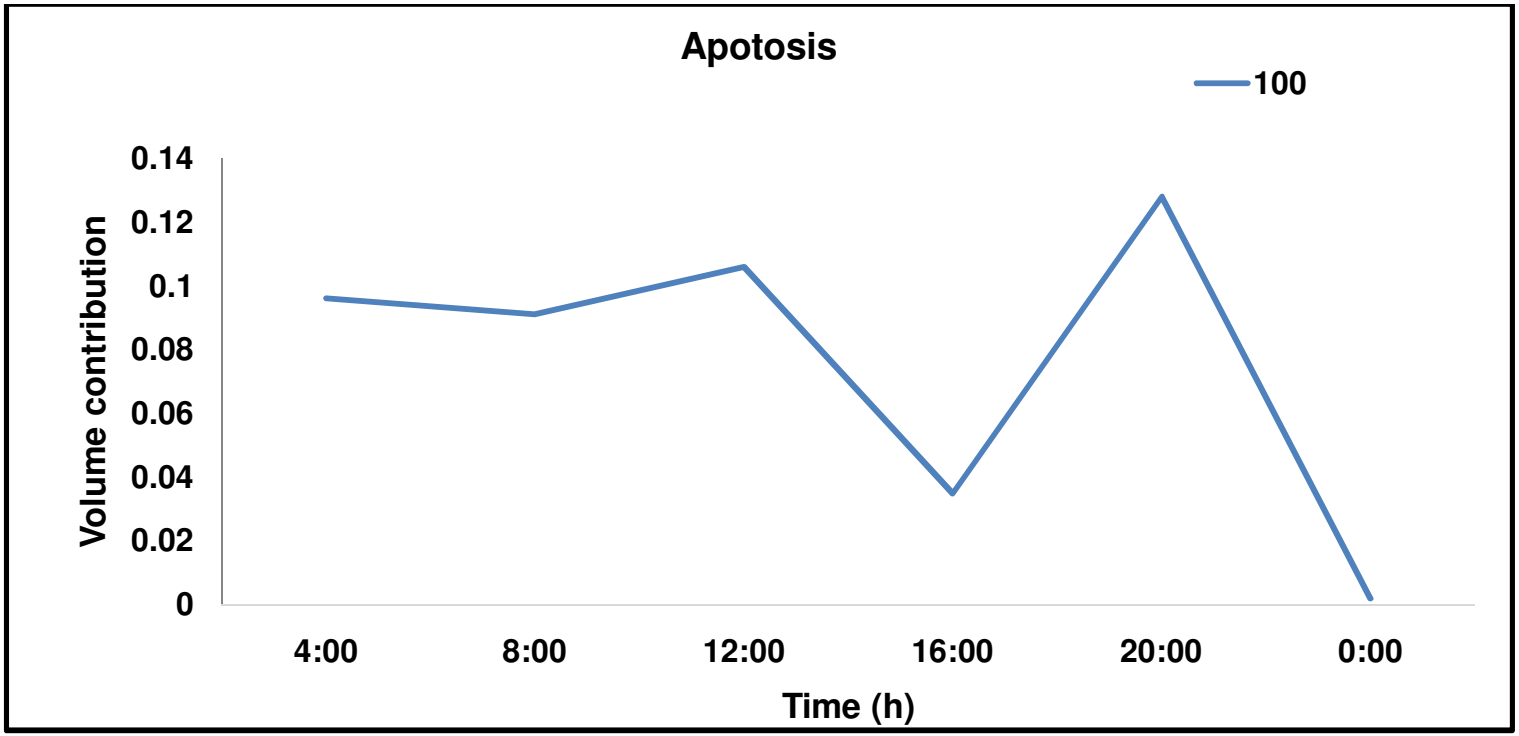

PeerJ PrePrints | https://doi.org/10.7287/peerj.preprints.1677v1 | CC-BY 4.0 Open Access | rec: 23 Jan 2016, publ: 23 Jan 2016

(H)

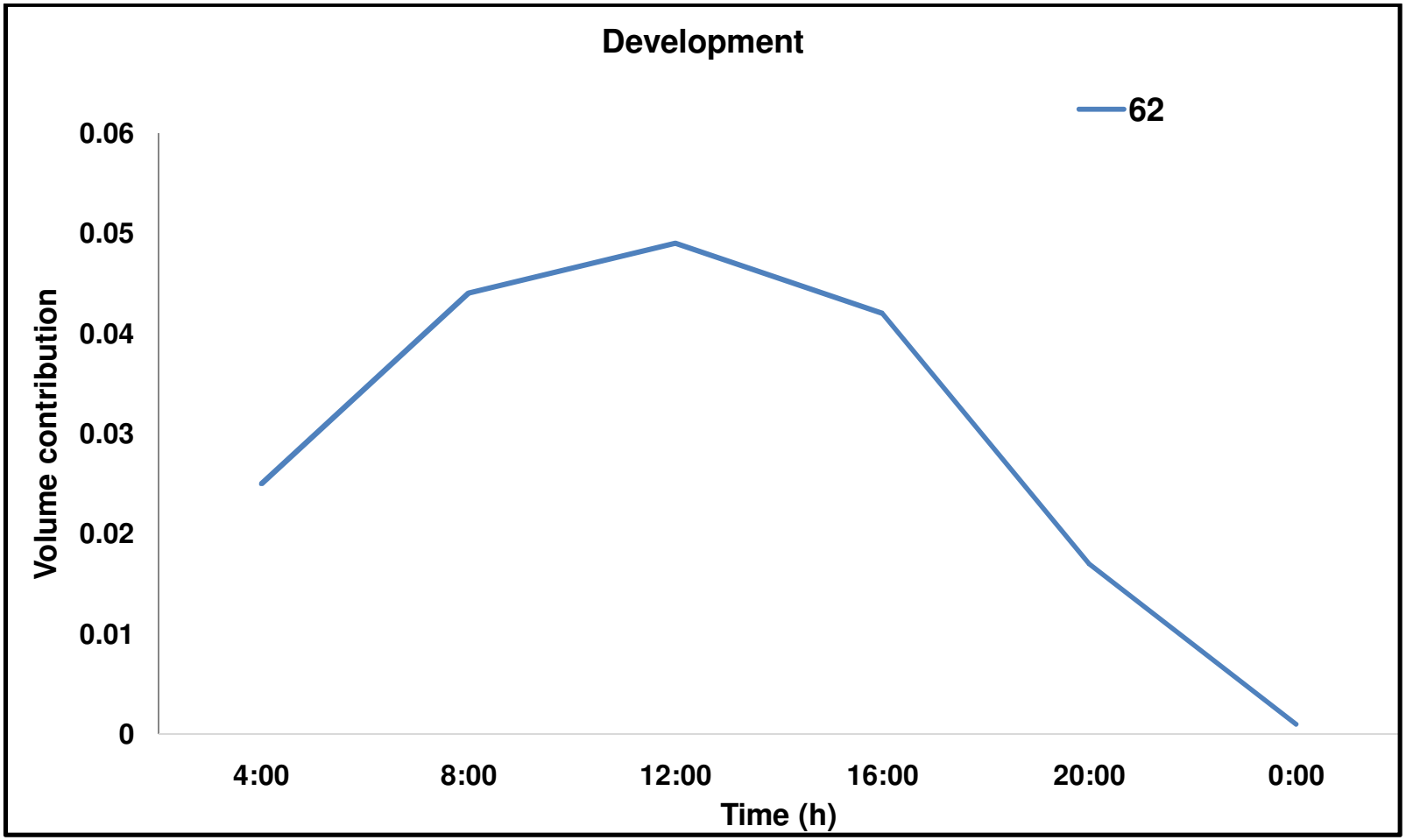

PeerJ PrePrints | https://doi.org/10.7287/peerj.preprints.1677v1 | CC-BY 4.0 Open Access | rec: 23 Jan 2016, publ: 23 Jan 2016

(I)

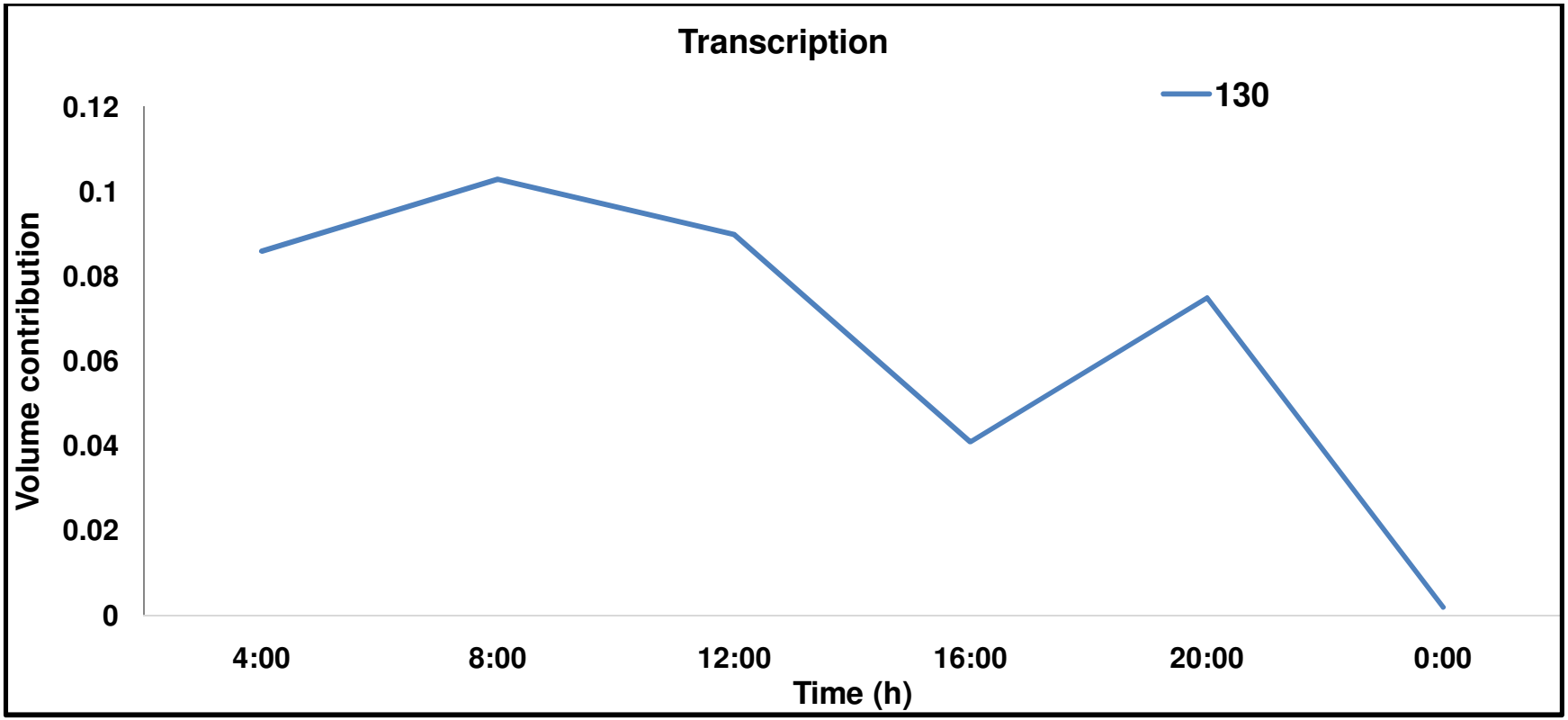

PeerJ PrePrints | https://doi.org/10.7287/peerj.preprints.1677v1 | CC-BY 4.0 Open Access | rec: 23 Jan 2016, publ: 23 Jan 2016

Table 1(on next page)

Table 1 Identification of *D. melanogaster* proteins.

Table 1 Identification of *Drosophila melanogaster* proteins that were differentially expressed by mass spectrometry. The MS data acquired was searched in Swiss-Prot database and the proteins were identified using the MASCOT search engine. The proteins are categorized into 11 groups based on known or predictive functions.

PeerJ PrePrints | https://doi.org/10.7287/peerj.preprints.1677v1 | CC-BY 4.0 Open Access | rec: 23 Jan 2016, publ: 23 Jan 2016

Table 1 Identification of *Drosophila melanogaster* proteins that were differentially expressed by mass spectrometry. The MS data acquired was searched in Swiss-Prot database and the proteins were identified using the MASCOT search engine. The proteins are categorized into 11 groups based on known or predictive functions.

S. No.	Spot/ Cluster ID/No.	Protein identification	Primary accession number	Theoretical Mass (Da)	Calculated pI	Peptide Score	No. of Peptides Matched	Sequence Coverage (%)
		Metabolism						
1	12	6-phosphofructokinase	P52034	86593	6.41	43	3	5
2	25	Succinate dehydrogenase	Q94523	72297	6.65	149	10	21
3	32	N-glycanase	Q28YQ7	73443	8.15	26	1	3
4	41	Maltase H	P07190	66344	4.75	82	5	10
5	44	Vacuolar ATP synthase catalytic subunit A	Q27331	68259	5.23	148	13	22
6	51	Vacuolar ATP synthase subunit B	P31409	54515	5.25	131	10	27
7	61	Enolase	P15007	54276	8.68	415	11	32
8	63	Phosphoglycerate kinase	Q01604	43834	7.01	223	6	18
9	64	ATP synthase subunit α	AC P35381	59384	9.09	332	5	15
10	68	Arginine kinase	P48610	39841	6.04	363	7	26

11	69	Fructose bisphosphate aldolase	P07764	39023	6.97	525	10	34
12	71	Arginine kinase	P48610	39841	6.04	291	10	38
13	72	Glyceraldehyde-3-phosphate dehydrogenase	P07486	35328	8.26	46	2	8
14	74	Glyceraldehyde-3-phosphate dehydrogenase	P07486	35328	8.26	332	5	25
15	75	Glyceraldehyde-3-phosphate dehydrogenase 1	P07486	35328	6.44	306	3	15
16	79	Alcohol dehydrogenase	P00334	27744	7.64	358	6	43
17	80	Stellate protein CG33247	Q7KV23	19396	7.64	28	1	5
18	81	Stellate protein CG33247	Q7KV23	19396	7.64	28	1	5
19	83	Triosephosphate isomerase	Q7JNS1	26609	6	178	7	43
20	90	ATP synthase subunit β	Q05285	54074	5.14	67	5	8
21	97	ATP synthase D chain	Q24251	20188	6.1	81	5	33
22	98	Tyrosine kinase 2	Q9V3D5	79559	9.13	23	1	1
23	105	ATP synthase subunit β	Q05825	54074	5.14	178	7	16
24	111	Protein l(2)37Cc	P18432	23700	4.67	56	1	6

25	117/118	ATP synthase subunit β	Q05825	54074	5.14	573	11	28
26	123	ATP synthase subunit β	Q05825	54074	5.14	61	6	17
27	124	Inorganic pyrophosphatase	O77460	37915	6.52	99	3	12
28	126	ATP synthase subunit β	Q05825	54074	5.14	48	2	3
29	131	Fructose bisphosphate aldolase	P07764	39023	6.97	92	5	21
30	132	Alcohol dehydrogenase	P00334	27744	7.74	198	5	28
31	133	Pyruvate kinase	O62619	57404	7.13	59	3	7
32	140	Phosphoglycerate kinase	Q01604	43834	7.01	195	7	15
33	152	Phosphoglycerate kinase	Q01604	43834	7.01	217	5	15
34	155	Glycerol-3-phosphate dehydrogenase	P13706	39659	6.17	96	7	26
35	156	Isocitrate dehydrogenase	Q9VWH4	40818	6.96	63	7	21
36	157	Glyceraldehyde-3-phosphate dehydrogenase	P07486	35328	8.26	106	2	8
37	159	ATP synthase subunit α	P35381	59384	9.09	380	10	20
38	161	Thioredoxin reductase I	P91938	64282	8.11	79	7	12
39	162	Fructose bisphosphate aldolase	P07764	39023	6.97	55	3	16

PeerJ PrePrints | https://doi.org/10.7287/peerj.preprints.1677v1 | CC-BY 4.0 Open Access | rec: 23 Jan 2016, publ: 23 Jan 2016

40	163	Alcohol dehydrogenase	P00334	27744	7.74	105	3	18
41	165	ATP synthase subunit α	P35381	59384	9.09	196	5	14
42	166	Maltase	P07190	66344	4.75	92	7	15
43	170	Pyruvate kinase	O62619	57404	7.13	35	2	4
44	171	Glycerol-3-phosphate dehydrogenase	Q27556	38298	6.33	27	6	20
45	173	ATP synthase subunit β	Q05825	54074	5.14	263	7	14
46	177	Fructose bisphosphate aldolase	P07764	39023	6.97	22	7	22
47	178	ATP synthase subunit α	P35381	59384	9.09	77	3	6
48	183	Alcohol dehydrogenase	P00334	27744	7.74	22	1	7
49	185	ATP synthase subunit β	Q05825	54074	5.14	32	1	2
50	186	Fructose bisphosphate aldolase	P07764	39023	6.97	176	6	16
51	187	Fructose bisphosphate aldolase	P07764	39023	6.97	107	4	13
52	192	Glyceraldehyde-3-phosphate dehydrogenase 1	P07486	35328	8.26	40	3	12
53	193	Cytochrome P450	Q9VGB5	55583	9.39	27	2	2
54	195	Fructose bisphosphate aldolase	P07764	39023	6.97	62	4	15
55	196	Fructose bisphosphate aldolase	P07764	39023	6.97	58	4	17

56	199	Inorganic pyrophosphatase	O77460	37915	6.52	93	5	19
57	209	Arginine kinase	P48610	39841	6.04	50	1	2
		Muscle activity						
58	57	Actin-87E	P10981	41775	5.3	132	6	20
59	59	Actin-88F	P83967	41673	5.29	421	7	26
60	94	Myosin light chain alkali	P06742	17513	4.29	89	2	16
61	102	Actin-57B	P53501	41808	5.23	22	5	17
62	104	Actin-88F	P83967	41673	5.29	413	5	22
63	106	Actin-5C	P10987	41795	5.3	27	2	6
64	114	Myosin regulatory light chain-2	P10987	41795	5.3	215	6	20
65	115	Actin-5C	P02574	41760	5.3	194	4	14
66	116	Actin-79B	Q540X7	41760	5.3	194	4	14
67	125	Actin-5C	P10987	41795	5.3	30	2	6
68	135	Actin-88F	P83967	41673	5.29	316	6	20
69	136	Actin-5C	P10987	41795	5.3	25	2	5
70	149	Actin-5C	P10987	41795	5.3	182	3	11
71	151	Synapse associated protein	Q960T2	56946	4.45	46	1	1

72	153	Actin-5C	P10987	41795	5.3	27	1	2
73	154	Tubulin α-1 chain	P06603	49876	5	173	5	14
74	158	ADP-ribosylation factor-8	Q9VHV5	21240	6.74	28	1	4
75	168	Actin-79B	P02574	41760	5.3	190	8	23
76	169	Actin-88F	P83967	41673	5.29	43	2	9
77	172	Tubulin β-1 chain	Q24560	50115	4.76	30	2	3
78	174	Actin-57B	P53501	41808	5.23	117	3	10
79	182	Actin-87E	P10981	41775	5.3	46	2	7
80	184	Actin-57B	P53501	41808	5.23	136	5	15
81	188	Actin-57B	P53501	41808	5.23	103	5	17
82	189	Actin-5C	P10987	41795	5.3	108	4	14
83	191	Actin-42A	P02572	41797	5.3	41	2	7
84	194	Tubulin α-3 chain	P06605	49859	5	78	1	3
85	198	Actin-79B	P83967	41760	5.29	118	5	20
86	200	Actin-87E	P10981	41775	5.3	194	5	20
87	201	Actin-57B	P53501	41808	5.23	112	3	10

88	202	Paramyosin	P35415	102277	5.47	36	5	7
89	203	Actin-42A	P02572	41797	5.3	83	2	6
90	208	Actin-5C	P10987	41795	5.3	45	3	9
		Heat shock proteins						
91	31	Heat shock 82 kDa protein	P02828	81814	4.91	23	4	9
92	42	Heat shock 70 kDa protein	P29844	72216	5.22	84	6	12
93	43	Heat shock 70 kDa protein	P11147	71087	5.36	188	8	16
94	46	Heat shock 60 kDa protein	O02649	60771	5.38	26	1	1
95	180	Heat shock factor protein	P22813	76886	4.87	27	1	3
		Ion-channel/cellular transport						
96	54	Calreticulin	P29413	46779	4.4	89	2	5
97	55	Tubulin β-1 chain	Q24560	50115	4.76	149	9	19
98	78	Voltage-dependent anion-selective channel (Porin)	Q94920	30531	7.74	387	7	36
99	96	Calcium-transporting ATPase	P22700	111630	5.28	27	1	1
100	160	ADP/ATP translocase	Q26365	34193	9.82	247	6	14
101	181	Voltage-dependent anion-selective channel (Porin)	Q94920	30531	6.44	195	4	20

102	205	Voltage-dependent anion-selective channel (Porin)	Q94920	30531	6.44	22	1	3
103	206	Voltage-dependent anion-selective channel (Porin)	Q94920	30531	6.44	27	1	3
104	207	Transient receptor potential locus C protein	P36951	29075	6.07	24	2	11
		Redox homeostasis						
105	85	Capon-like protein	Q8SXX4	77233	8.98	22	1	1
106	86	Superoxide dismutase [Cu-Zn]	P61851	15689	5.67	162	8	62
107	120	Glutathione-S-transferase	P41043	27596	4.57	224	5	19
108	134	Catalase	ACP17336	57113	8.39	54	4	9
109	175	Superoxide dismutase [Cu-Zn]	P61851	15689	5.67	56	3	24
110	197	Glutathione-S-transferase	P41043	27596	4.57	74	3	9
111	204	Glutathione-S-transferase	P20432	23851	6.75	61	1	4
		Protein synthesis/folding/degradation						
112	50	Protein disulfide isomerase	P54399	55746	4.72	65	2	5
113	99	Furin-like protease	P30430	120917	6.25	22	1	1

114	121	40S ribosomal protein SA	P38979	30209	4.76	50	2	9
115	164	Elongation factor 1α (EF-1α)	P08736	59384	9.09	52	4	9
116	167	40S ribosomal protein SA	P38979	30209	4.76	38	2	9
117	179	40S ribosomal protein S12	P80455	15159	5.93	32	1	10
		Apoptosis						
118	100	Thioredoxin peroxidase	Q9V3P0	21724	5.52	122	4	26
119	176	Caspase-8 precursor	Q29IM7	57539	6.31	22	1	3
		Development						
120	62	Vitellogenin-2 precursor	AC P02844	49630	7.74	56	6	12
121	87	Protein stand still	P92189	35753	9.28	26	1	2
		Replication						
122	190	DNA polymerase α - catalytic subunit	P26019	169796	8.28	33	1	0
		Transcription						
123	130	RNA helicase	Q6J5K9	144797	5.67	30	1	0
		Cell division						
124	38	Mitosis initiation protein fs(1)Ya	P25028	77677	9.54	21	1	2

7

Table 2(on next page)

Table 2 Expression levels of proteins as percentage of volume contribution.

Table 2 Expression levels of proteins as percentage of volume contribution by image analysis (ImageMaster 2D Platinum software, version 7.0). The proteins in the groups (metabolism, muscle activity, ion-channel/cellular transport, heat shock, protein synthesis/folding/degradation, redox homeostasis, apoptosis, development and transcription) which show significant variation in at least 2 time points are included in the table. At each time point, 2-DE was performed in triplicate. For other details see Supplemental Table 1.

Table 2 Expression levels of proteins as percentage of volume contribution by image analysis (ImageMaster 2D Platinum software, version 7.0). The proteins in the groups (metabolism, muscle activity, ion-channel/cellular transport, heat shock, protein synthesis/folding/degradation, redox homeostasis, apoptosis, development and transcription) which show significant variation in at least 2 time points are included in the table. At each time point, 2-DE was performed in triplicate. For other details see Supplemental Table 1.

S. No.	Spot/ Cluster ID/No.	Protein Name	Significance level of % volume[a]					
			04:00	08:00	12:00	16:00	20:00	00:00
		Metabolism						
1	12	6-phosphofructokinase	0.0168 ± 0.080		0.013871 ± 0.0093 p = 0.00017[c]		0.00355 ± 0.00336 p = 0.00026[d]	
2	25	Succinate dehydrogenase	0.05666 ± 0.03670			0.01156 ± 0.01067 p = 6.8929E-05[b]	0.02717 ± 0.01942 p = 0.00980[d]	
3	32	N-glycanase	0.04920 ± 0.02726		0.02594 ± 0.01233 p = 0.00870[b]	0.00113 ± 0.00013 p = 2.5021E-05[c]	0.00715 ± 0.00467 p = 6.7294E-07[d]	
4	41	Maltase H	0.03721 ± 0.02519	0.04786 ± 0.06067	0.03036 ± 0.01416	0.01673 ± 0.01416	0.0195 ± 0.01690	0.000583 ± 0.00065 p = 0.00036[b] p = 0.00233[c]
5	44	Vacuolar ATP synthase catalytic subunit A	0.00312 ± 0.02442	0.03587 ± 0.06408	0.04102 ± 0.03517	0.01178 ± 0.01333	0.02862 ± 0.01673	0.0080 ± 0.0015 p = 0.00771[b] p = 0.00177[c]
6	51	Vacuolar ATP synthase	0.08049 ±		0.06707 ±		0.04721 ±	0.01295 ±

		catalytic subunit B	0.05789		0.03213 $p = 0.00198^{c}$		0.01989	0.00224 $p = 7.1834E\text{-}05^{b}$ $p = 0.00198^{c}$
7	61	Enolase	0.03289 ± 0.00521	0.05179 ± 0.07539	0.09340 ± 0.08054 $p = 0.00139^{b}$	0.12059 ± 0.11632 $p = 0.00239^{b}$	0.0561 ± 0.07604	0.00145 ± 0.00177
8	64	ATP synthase subunit α	0.01221 ± 0.01438	0.07412 ± 0.00754 $p = 7.3863E\text{-}08^{b}$ $p = 5.7179E\text{-}06^{c}$	0.01719 ± 0.0472	0.02236 ± 0.04303	0.01559 ± 0.00272	0.0345 ± 0.02371
9	69	Fructose bisphosphate aldolase	0.02904 ± 0.00464	0.05306 ± 0.03179	0.10312 ± 0.00128 $p = 0.00186^{b}$ $p = 0.00093^{c}$	0.0154 ± 0.0300	0.02551 ± 0.00406	0.05898 ± 0.02373
10	71	Arginine kinase	0.12971 ± 0.07577		0.13765 ± 0.02036 $p = 0.00838^{c}$		0.04893 ± 0.04735	0.00027 ± 0.00018 $p = 0.0010^{b}$
11	80	Stellate protein CG33247	0.01139 ± 0.00267	0.0197 ± 0.0438	0.05522 ± 0.01000 $p = 0.00483^{b}$	0.0296 ± 0.0644	0.00743 ± 0.01502	0.00266 ± 0.00303
12	81	Stellate protein CG33247	0.00784 ± 0.00121	0.02921 ± 0.0239	0.05163 ± 0.00106 $p = 0.00507^{b}$	0.01766 ± 0.0354	0.0129 ± 0.02987	0.00360 ± 0.00349
13	83	Triosephosphate isomerase	0.01722 ± 0.07347	0.01545 ± 0.06742	0.10425 ± 0.08459	0.11867 ± 0.08459	0.12435 ± 0.02904	0.02646 ± 0.01363 $p = 0.00061^{c}$
14	90	ATP synthase subunit β	0.0121 ± 0.00155			0.00539 ± 0.00112 $p = 0.00247^{b}$	0.019 ± 0.03214 $p = 0.00024^{d}$	
15	97	ATP synthase D chain	0.08024 ± 0.01850	0.04083 ± 0.0364	0.05072 ± 0.04827	0.03286 ± 0.02797	0.06776 ± 0.06139	0.01847 ± 0.00439 $p = 0.00263^{b}$

16	105	ATP synthase subunit β	0.06354 ± 0.05091	0.01256 ± 0.03672	0.04666 ± 0.05516	0.0397 ± 0.02289	0.02342 ± 0.03046	0.00179 ± 0.00281 $p = 0.00151^{b}$
17	111	Protein l(2)37Cc	0.06736 ± 0.04438	0.018423 ± 0.00270 $p = 0.00809^{b}$	0.05768 ± 0.02585	0.07649 ± 0.10300	0.0401 ± 0.03811	0.00559 ± 0.00881 $p = 0.00022^{b}$ $p = 0.00787^{c}$
18	117	ATP synthase subunit β	0.05724 ± 0.00662	0.02367 ± 0.0637	0.07744 ± 0.09473	0.0326 ± 0.06556	0.0476 ± 0.0820	0.00466 ± 0.00134 $p = 0.00096^{b}$
19	123	ATP synthase subunit β	0.01906 ± 0.01613	0.00331 ± 0.00433	0.02062 ± 0.0099	0.01013 ± 0.0012	0.03737 ± 0.02032	0.00281 ± 0.00336 $p = 0.00080^{c}$
20	124	Inorganic pyrophosphatase	0.03386 ± 0.02401	0.0325 ± 0.01715	0.04636 ± 0.02574	0.02309 ± 0.02131	0.05833 ± 0.00977	0.00568 ± 0.00112 $p = 0.00721^{b}$ $p = 1.5608\text{E-}06^{c}$
21	131	Fructose bisphosphate aldolase	0.05415 ± 0.05416	0.01170 ± 0.02879 $p = 0.00780^{c}$	0.03636 ± 0.01339	0.0522 ± 0.07434	0.0694 ± 0.00939	0.054637 ± 0.00665
22	133	Pyruvate kinase	0.05199 ± 0.03744	0.0145 ± 0.01690	0.0377 ± 0.0492	0.01838 ± 0.01070 $p = 0.00287^{b}$		
23	152	Phosphoglycerate kinase	0.08607 ± 0.05137	0.17323 ± 0.03216	0.14976 ± 0.02226	0.34022 ± 0.07880 $p = 0.00945^{b}$	0.13099 ± 0.00249	0.01186 ± 0.00197 $p = 0.00016^{c}$
24	155	Glycerol-3-phosphate dehydrogenase	0.03523 ± 0.01054	0.0993 ± 0.05331	0.03185 ± 0.01802	0.01244 ± 0.00796	0.00780 ± 0.00056 $p = 0.00706^{d}$	0.00171 ± 0.00257 $p = 1.6430\text{E-}05^{b}$ $p = 0.00440^{c}$
25	156	Isocitrate dehydrogenase	0.09404 ± 0.06044	0.02818 ± 0.00736	0.03816 ± 0.0096	0.02102 ± 0.06067	0.06589 ± 0.10657	0.00184 ± 0.00023 $p = 5.3619\text{E-}05^{b}$

26	157	Glyceraldehyde-3-phosphate dehydrogenase	0.03387± 0.00190	0.17997 ± 0.03068 $p = 0.00119^{b}$			0.11537 ± 0.00203 $p = 9.0253E\text{-}07^{d}$	
27	161	Thioredoxin reductase I	0.06182 ± 0.03565	0.01353 ± 0.01329	0.15359 ± 0.05446 $p = 0.00536^{c}$	0.04874 ± 0.01566	0.01517 ± 0.00499	0.00059 ± 0.00048 $p = 0.00265^{b}$ $p = 0.00012^{c}$
28	162	Fructose bisphosphate aldolase	0.03210 ± 0.01170	0.02430 ± 0.01086 $p = 0.00021^{c}$	0.06483 ± 0.01934 $p = 0.00315^{b}$ $p = 0.00938^{c}$	0.07216 ± 0.02846 $p = 0.00248^{b}$	0.12061 ± 0.00710 $p = 4.1997E\text{-}08^{d}$	0.01689 ± 0.00260 $p = 0.00263^{c}$
29	163	Alcohol dehydrogenase				0.04532 ± 0.01706 $p = 0.00964^{c}$	0.00838 ± 0.00187	
30	165	ATP synthase subunit α	0.06259 ± 0.02558	0.05752 ± 0.04504	0.01409 ± 0.01	0.09364 ± 0.01434	0.0328 ± 0.00413	0.00082 ± 0.00054 $p = 0.00123^{b}$
31	166	Maltase H	0.00333 ± 0.00325	0.08944 ± 0.09212	0.00040 ± 0.00019 $p = 0.00216^{c}$	0.00617 ± 0.00298	0.00480 ± 0.00155	0.04754 ± 0.03454
32	170	Pyruvate kinase	0.00480 ± 0.00251				0.02907 ± 0.00478 $p = 0.00839^{d}$	
33	171	Glycerol-3-phosphate dehydrogenase	0.01344 ± 0.00408	0.00372 ± 0.00255 $p = 0.00016^{c}$	0.00526 ± 0.00287 $p = 0.00020^{c}$	0.00482 ± 0.00032 $p = 0.00736^{b}$	0.05168 ± 0.00546 $p = 0.00063^{d}$	0.00688 ± 0.00578 $p = 0.00063^{b}$
34	173	ATP synthase subunit β			0.00046 ± 0.00031 $p = 0.00025^{c}$	0.15433 ± 0.02157 $p = 0.00126^{c}$	0.04854 ± 0.00678	
35	177	Fructose bisphosphate aldolase	0.00406 ± 0.00075			0.00050 ± 0.00027 $p = 0.00153^{b}$ $p = 0.00030^{c}$	0.04982 ± 0.00730 $p = 0.00041^{d}$	
36	178	ATP synthase subunit α	0.00288 ±			0.00459 ±	0.05003 ±	

			0.00394			0.00615 $p = 0.00025^{c}$	0.00671 $p = 3.2629E\text{-}06^{d}$	
37	185	ATP synthase subunit β	0.00871 ± 0.00543		0.01777 ± 0.00956 $p = 1.7782E\text{-}06^{c}$	0.04401 ± 0.01014 $p = 0.00020^{b}$ $p = 0.00029^{c}$	0.09301 ± 0.00422 $p = 5.0701E\text{-}09^{d}$	0.00877 ± 0.00187 $p = 1.0732E\text{-}05^{c}$
38	186	Fructose bisphosphate aldolase	0.10034 ± 0.05736	0.00754 ± 0.01134 $p = 2.2442E\text{-}07^{b}$	0.06666 ± 0.02744 $p = 0.00087^{c}$	0.05637 ± 0.02768 $p = 0.00536^{c}$	0.00989 ± 0.02621 $p = 5.4053E\text{-}06^{d}$	
39	187	Fructose bisphosphate aldolase	0.01225 ± 0.01942	0.09305 ± 0.03952 $p = 0.00727^{b}$	0.02897 ± 0.01348 $p = 0.00241^{c}$	0.02634 ± 0.04315 $p = 0.00226^{c}$	0.15707 ± 0.06963 $p = 0.00277^{d}$	0.00230 ± 0.00212 $p = 2.0640E\text{-}05^{c}$
40	193	Cytochrome P450	0.00662 ± 0.00730		0.00985 ± 0.00105 $p = 0.00174^{b}$ $p = 0.00028^{c}$	0.02990 ± 0.00493 $p = 0.00012^{c}$	0.05572 ± 0.00066 $p = 1.0684E\text{-}06^{d}$	
41	195	Fructose bisphosphate aldolase	0.00581 ± 0.00388	0.03529 ± 0.05554	0.02590 ± 0.00795 $p = 0.00391^{b}$	0.04218 ± 0.00960 $p = 0.00090^{b}$	0.02665 ± 0.02258	0.00053 ± 0.00047 $p = 0.00139^{b}$ $p = 0.00307^{c}$
42	199	Inorganic pyrophosphatase	0.02621 ± 0.01431				0.04274 ± 0.01619	0.00144 ± 0.00105 $p = 1.0825E\text{-}06^{b}$ $p = 5.2773E\text{-}09^{c}$
43	209	Arginine kinase	0.01591 ± 0.00931	0.04940 ± 0.01749 $p = 0.00610^{b}$	0.07943 ± 0.01468 $p = 2.8958E\text{-}05^{b}$	0.079384 ± 0.03733 $p = 0.00411^{b}$	0.05711 ± 0.00992 $p = 0.00047^{d}$	0.00402 ± 0.00257 $p = 0.00013^{c}$
		Muscle activity						
44	59	Actin-88F	0.02046 ± 0.00313	0.06569 ± 0.00868 $p = 5.8021E\text{-}05^{b}$	0.0269 ± 0.07303	0.01924 ± 0.04082	0.01591 ± 0.02909	0.0039 ± 0.00216 $p = 1.1928E\text{-}06^{b}$ $p = 1.1046E\text{-}05^{c}$
45	102	Actin-57B	0.07233 ± 0.01558		0.02407 ± 0.01990 $p = 0.00101^{b}$		0.05179 ± 0.02690	0.00096 ± 0.00085 $p = 5.0262E\text{-}07^{b}$ $p = 0.00038^{c}$

46	104	Actin-88F	0.11418 ± 0.01078	0.12801 ± 0.01392	0.14641 ± 0.11335	0.0227 ± 0.00535 p = 0.00738[b] p = 0.00032[c]	0.18435 ± 0.17218	0.04722 ± 0.03402
47	114	Myosin regulatory light chain-2	0.03078 ± 0.00338	0.00768 ± 0.02413	0.02481 ± 0.08161	0.02176 ± 0.05122	0.0174 ± 0.0255	0.00723 ± 0.00110 p = 0.00103[b]
48	115	Actin-5C	0.02452 ± 0.00371	0.00461 ± 0.00065 p = 0.00750[b]	0.02079 ± 0.0455	0.00308 ± 0.00072 p = 4.9214E-05[b]	0.00398 ± 0.00122 p = 0.00549[d]	0.00535 ± 0.00147 p = 0.00911[b]
49	116	Actin-79B	0.06538 ± 0.00565	0.00187 ± 0.00272 p = 7.981E-06[b] p = 0.00435[c]	0.02916 ± 0.08442	0.00724 ± 0.00169 p = 1.6044E-07[b]	0.01044 ± 0.00186 p = 2.6139E-06[d]	0.00615 ± 0.00132 p = 3.6987E-07[b]
50	149	Actin-5C	0.05339 ± 0.03502	0.04162 ± 0.0414	0.05021 ± 0.04663	0.15640 ± 0.19589	0.0328 ± 0.04848	0.00433 ± 0.00909 p = 0.00601[b]
51	151	Synapse associated protein			0.01538 ± 0.0055 p = 0.00118[c]	0.00974 ± 0.00762 p = 0.00132[c]	0.03087 ± 0.00508	
52	158	ADP-ribosylation factor-8	0.06229 ± 0.03123	0.01840 ± 0.00531 p = 0.00325[c]	0.10726 ± 0.01584	0.16042 ± 0.06361	0.09388 ± 0.02007	0.00920 ± 0.00118 p = 0.00746[b] p =0.00025[c]
53	168	Actin-79B	0.00114 ± 0.00188		0.0201 ± 0.02050 p = 0.00921[b]		0.02964 ± 0.01304 p = 2.1258E-05[d]	
54	169	Actin-88F	0.00256 ± 0.00179				0.04922 ± 0.02446 p = 0.00191[d]	
55	174	Actin-57B	0.00193 ± 0.00344			0.04580 ± 0.01204 p = 0.00085[b]	0.03273 ± 0.00470 p = 0.00016[d]	0.00812 ± 0.00773 p = 0.00102[c]
56	182	Actin-87E	0.00355 ± 0.00395			0.05350 ± 0.03246 p = 0.00520[b]	0.07146 ± 0.01176 p = 9.2309E-07[d]	

57	184	Actin-57B	0.00062 ± 0.00095			0.12755 ± 0.00720 p = 1.3775E-07[b] p = 3.7756E-05[c]	0.0122 ± 0.02055	
58	188	Actin-57B	0.05530 ± 0.01465	0.14250 ± 0.00663 p = 0.00071[b] p = 4.5473E-05[c]	0.08487 ± 0.05086	0.09601 ± 0.01685 p = 0.00666[c]	0.04235 ± 0.00629	0.0421 ± 0.07126
59	189	Actin-5C	0.05170 ± 0.00922	0.27330 ± 0.07415 p = 0.00680[b] p = 0.00632[c]	0.11201 ± 0.05377	0.06672 ± 0.04820	0.0506 ± 0.0797	0.07088 ± 0.0666
60	194	Tubulin α-3 chain	0.00143 ± 0.00293		0.02587 ± 0.01795 p = 0.00082[b] p = 0.00204[c]	0.00259 ± 0.00353 p = 1.8164E-08[c]	0.07357 ± 0.00403 p = 8.0941E-09[d]	
61	198	Actin-79B	0.0135 ± 0.0029	0.05796 ± 0.00308 p = 5.6253E-05[b]		0.08917 ± 0.00759 p = 8.7657E-05[b]		
62	200	Actin-87E	0.0110 ± 0.01541	0.02004 ± 0.00506	0.05987 ± 0.00764 p = 0.00248[b]	0.06444 ± 0.05897	0.03010 ± 0.02593	0.00197 ± 0.00100 p = 0.00156[c]
63	201	Actin-57B					0.06669 ± 0.02571	0.00313 ± 0.00456 p = 4.3266E-05[c]
64	202	Paramyosin	0.01868 ± 0.00829	0.08292 ± 0.05254	0.05174 ± 0.00992 p = 0.00556[b]	0.15828 ± 0.04194 p = 0.00481[b]	0.04854 ± 0.0097	0.01727 ± 0.01595
65	203	Actin-42A		0.07337 ± 0.01193 p = 0.00736[c]			0.02297 ± 0.01262	
66	208	Actin-5C	0.03647 ± 0.01753	0.01795 ± 0.01412	0.04708 ± 0.01341	0.08915 ± 0.02907	0.03239 ± 0.00920	0.00092 ± 0.00019 p = 0.00407[c]

		Ion-channel/cellular transport						
67	54	Calreticulin	0.06318 ± 0.072311	0.07632 ± 0.01609	0.05745 ± 0.01702	0.02592 ± 0.01448 $p = 0.00454^{c}$	0.12495 ± 0.02609	0.0131 ± 0.00333 $p = 0.00012^{c}$
68	55	Tubulin β-1 chain	0.0158 ± 0.00237	0.00237 ± 0.0025	0.03131 ± 0.05206	0.06529 ± 0.00427 $p = 0.00053^{b}$ $p = 0.00834^{c}$	0.0227 ± 0.02573	0.00163 ± 0.00122
69	78	Voltage-dependent anion-selective channel (Porin)	0.0109 ± 0.01073	0.2164 ± 0.0563	0.1006 ± 0.1049	0.0921 ± 0.01156 $p = 0.00140^{b}$	0.13172 ± 0.11014	0.03589 ± 0.00776
70	160	ADP/ATP translocase	0.00215 ± 0.00150			0.0302 ± 0.02585 $p = 0.00012^{b}$ $p = 9.6783E\text{-}07^{c}$	0.00391 ± 0.00784	
71	206	Voltage-dependent anion-selective channel (Porin)	0.07494 ± 0.06443	0.0116 ± 0.04136	0.06563 ± 0.00627	0.076146 ± 0.02511	0.04800 ± 0.10300	0.00101 ± 0.00116 $p = 0.00581^{b}$
72	207	Transient receptor potential locus C protein				0.07783 ± 0.01334 $p = 0.00394^{c}$	0.02824 ± 0.00534	0.00036 ± 0.00019 $p = 4.0791E\text{-}08^{c}$
		Heat shock proteins						
73	31	Heat shock 82 kDa protein	0.02077 ± 0.01520		0.012483 ± 0.0060 $p = 1.7087E\text{-}05^{c}$		0.00111 ± 0.00014 $p = 0.00101^{d}$	
74	42	Heat shock 70 kDa protein	0.05238 ± 0.01099	0.00207 ± 0.00078 $p = 0.00012^{b}$	0.0305 ± 0.00145 $p = 0.00939^{b}$	0.00959 ± 0.00818 $p = 5.2107E\text{-}05^{b}$	0.02227 ± 0.01378 $p = 0.00187^{d}$	0.00374 ± 0.00089 $p = 1.62E\text{-}08^{b}$ $p = 0.00028^{c}$
75	43	Heat shock 70 kDa protein	0.05023 ± 0.04775	0.03493 ± 0.00646	0.04306 ± 0.02875 $p = 0.00157^{c}$	0.01095 ± 0.00139	0.01596 ± 0.01483 $p = 0.00948^{d}$	0.00101 ± 0.00228 $p = 8.70E\text{-}03^{b}$ $p = 8.95E\text{-}06^{c}$

76	46	Heat shock 60 kDa protein	0.05832 ± 0.03522	0.01751 ± 0.01643 $p = 0.00400^{b}$	0.02924 ± 0.01869	0.00205 ± 0.02335 $p = 0.00819^{b}$	0.00164 ± 0.00208 $p = 0.00080^{d}$	0.01227 ± 0.00143 $p = 0.00048^{b}$
77	180	Heat shock factor protein	0.01626 ± 0.00932				0.04055 ± 0.00227 $p = 0.00755^{d}$	
		Protein synthesis/folding/ degradation						
78	50	Protein disulfide isomerase	0.05850 ± 0.00582	0.00525 ± 0.000696	0.01486 ± 0.00272	0.01374 ± 0.01066	0.01429 ± 0.02467	0.00699 ± 0.00148 $p = 0.00237^{b}$
79	99	Furin-like protease	0.02738 ± 0.01222	0.04072 ± 0.01344	0.04672 ± 0.0098	0.05014 ± 0.00689 $p = 0.00352^{c}$	0.03017 ± 0.00327	0.2291 ± 0.00774
80	121	40S ribosomal protein SA	0.13683 ± 0.01787	0.02732 ± 0.01356 $p = 0.00107^{b}$ $p = 0.00908^{c}$	0.06246 ± 0.02463 $p = 0.00708^{b}$	0.00885 ± 0.00078 $p = 2.5433E\text{-}05^{b}$ $p = 2.0399E\text{-}08^{c}$	0.05494 ± 0.00225 $p = 0.00023^{d}$	0.00305 ± 0.00589 $p = 1.61E\text{-}06^{b}$ $p = 0.00022^{c}$
81	164	Elongation factor 1α (EF-1α)	0.01402 ± 0.01559	0.04487 ± 0.04267	0.03916 ± 0.03485	0.05944 ± 0.00664 $p = 0.00147^{b}$	0.06306 ± 0.00781 $p = 0.00098^{d}$	0.00452 ± 0.00442 $p = 2.9002E\text{-}09^{c}$
82	179	40S ribosomal protein S12	0.00028 ± 0.00028				0.08388 ± 0.00936 $p = 2.3206E\text{-}05^{d}$	
		Redox homeostasis						
83	197	Glutathione-S-transferase	0.01685 ± 0.00487	0.02996 ± 0.01557	0.01077 ±0.00323	0.08026 ± 0.02642	0.04748 ± 0.03732	0.00108 ± 0.00099 $p = 3.3424E\text{-}08^{b}$ $p = 0.00028^{c}$
84	204	Glutathione-S-transferase	0.05135 ± 0.03322	0.09755 ± 0.05312	0.02023 ± 0.02641	0.09738 ± 0.04084	0.04298 ± 0.01096	0.00243 ± 0.00236 $p = 0.00030^{b}$

								p = 1.1889E-07[c]
		Apoptosis						
85	100	Thioredoxin peroxidase	0.09598 ± 0.01127	0.09064 ± 0.10128	0.10623 ± 0.0569	0.03505 ± 0.01026 p = 0.00228[b] p = 8.085E-06[c]	0.12797 ± 0.00070 p = 0.00205[b]	0.00244 ± 0.00142 p = 1.2261E-06[b] p = 1.00E-07[c]
86	176	Caspase-8 precursor	0.00092 ± 0.00013		0.00133 ± 0.00074 p = 4.1969E-06[c]	0.00473 ± 0.00655 p = 1.77E-06[c]	0.04464 ± 0.00337 p = 0.00012[d]	
		Development						
87	62	Vitellogenin-2 precursor	0.02446 ± 0.00269	0.0436 ± 0.0398	0.04901 ± 0.02959 p = 0.00238[b] p = 0.00149[c]	0.0417 ± 0.05467	0.01699 ± 0.00314	0.00053 ± 0.00009
		Transcription						
88	130	RNA helicase	0.08621 ± 0.03634	0.10347 ± 0.0988	0.09000 ± 0.01469	0.04088 ± 0.01000 p = 0.00092[c]	0.07469 ± 0.00027	0.00160 ± 0.00133 p = 0.00046[b] p =0.00071[c]

[a] – values are expressed in mean±SD

[b] – value compared with 04:00

[c] – value compared with 20:00

[d] – comparison of 04:00 and 20:00